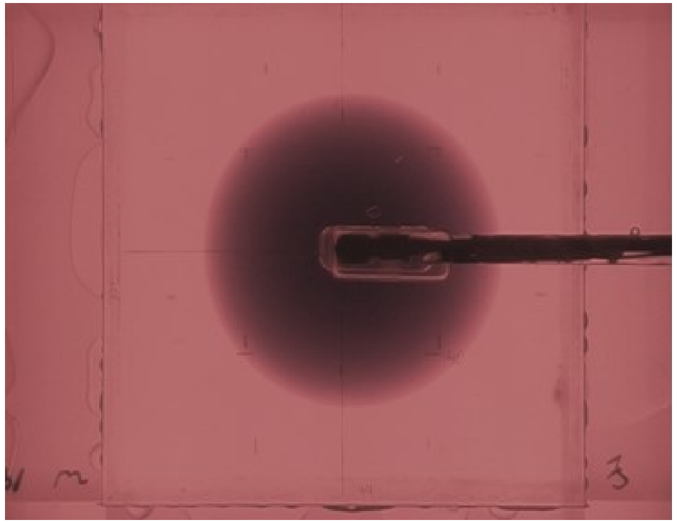

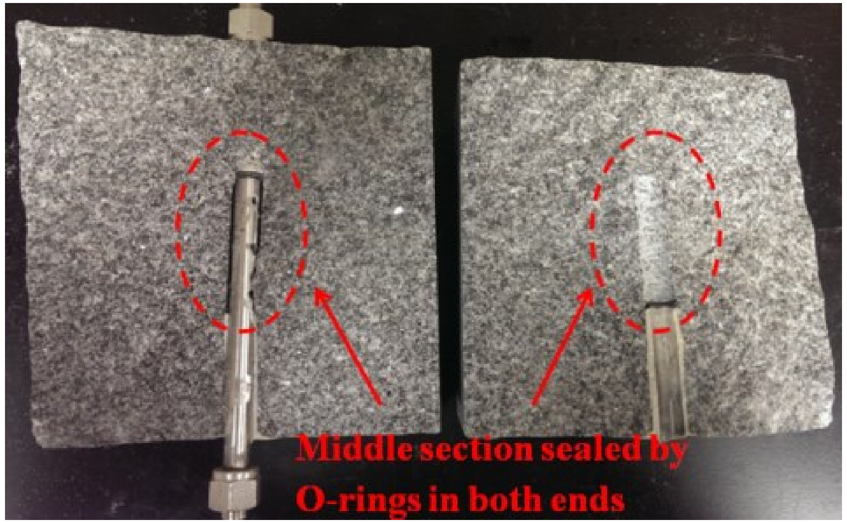

TIME DEPENDENCE AND WIDTH CONSTRICTION IN ROCK FRACTURE – EXPERIMENTAL EVIDENCE AND MODELING RESPONSES

Andrew Bunger

University of Pittsburgh, Pittsburgh, Pennsylvania

WFM2024, 6 March 2024, Baton Rouge, LA, USA

Bunger@pitt.edu

Modelling fluid-driven fracturing

Find

w = Crack opening

p_f = Fluid pressure p_f

$S(t)$ = Crack front location

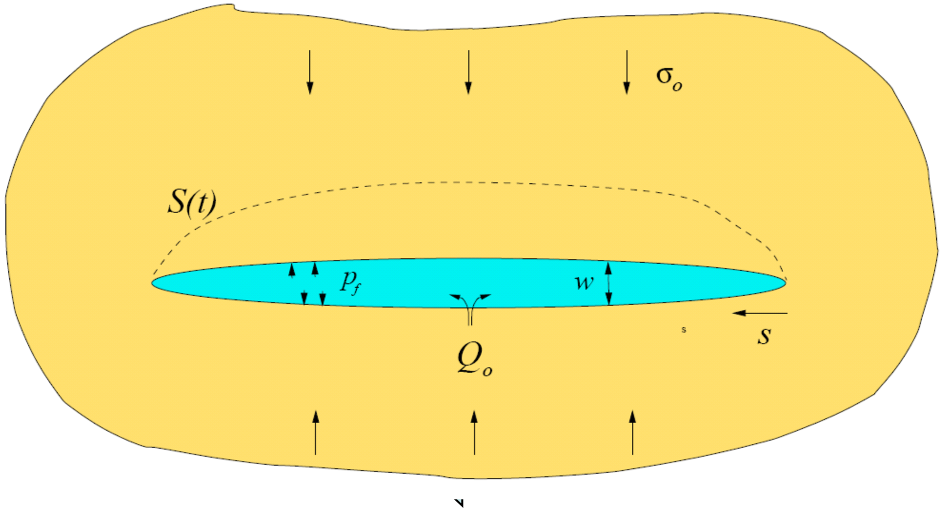

Elasticity Equation: $$p_{\mathrm{f}} - \sigma_o = -\frac{E'}{8\pi}\int_{C(t)} \frac{w(x',y',t)\,\mathrm{d}C(x',y')}{\left[(x'-x)^2+(y'-y)^2\right]^{3/2}}$$

Reynold's Lubrication Equation: $$\frac{\partial w}{\partial t} = \frac{1}{\mu'}\nabla\cdot\left(w^3\nabla p_{\mathrm{f}}\right) + Q_o\delta(x,y)$$

Propagation Condition: $$\lim_{s\to 0}\frac{w}{s^{1/2}} = \frac{K'}{E'}$$

Boundary Conditions: $$\lim_{s\to 0} w^3\frac{\partial p_{\mathrm{f}}}{\partial s} = 0$$

Coupled, non-linear, non-local system of PDEs with a moving boundary

$\mu' = 12\times$ Dynamic fluid viscosity

$E' =$ (Plane strain) Elastic modulus of the rock

$K' = \left(\frac{32}{\pi}\right)^{1/2}\times$ Fracture toughness of the rock

$Q_o =$ Fluid injection rate

LEFM and non-LEFM Tip Behavior in Experiments

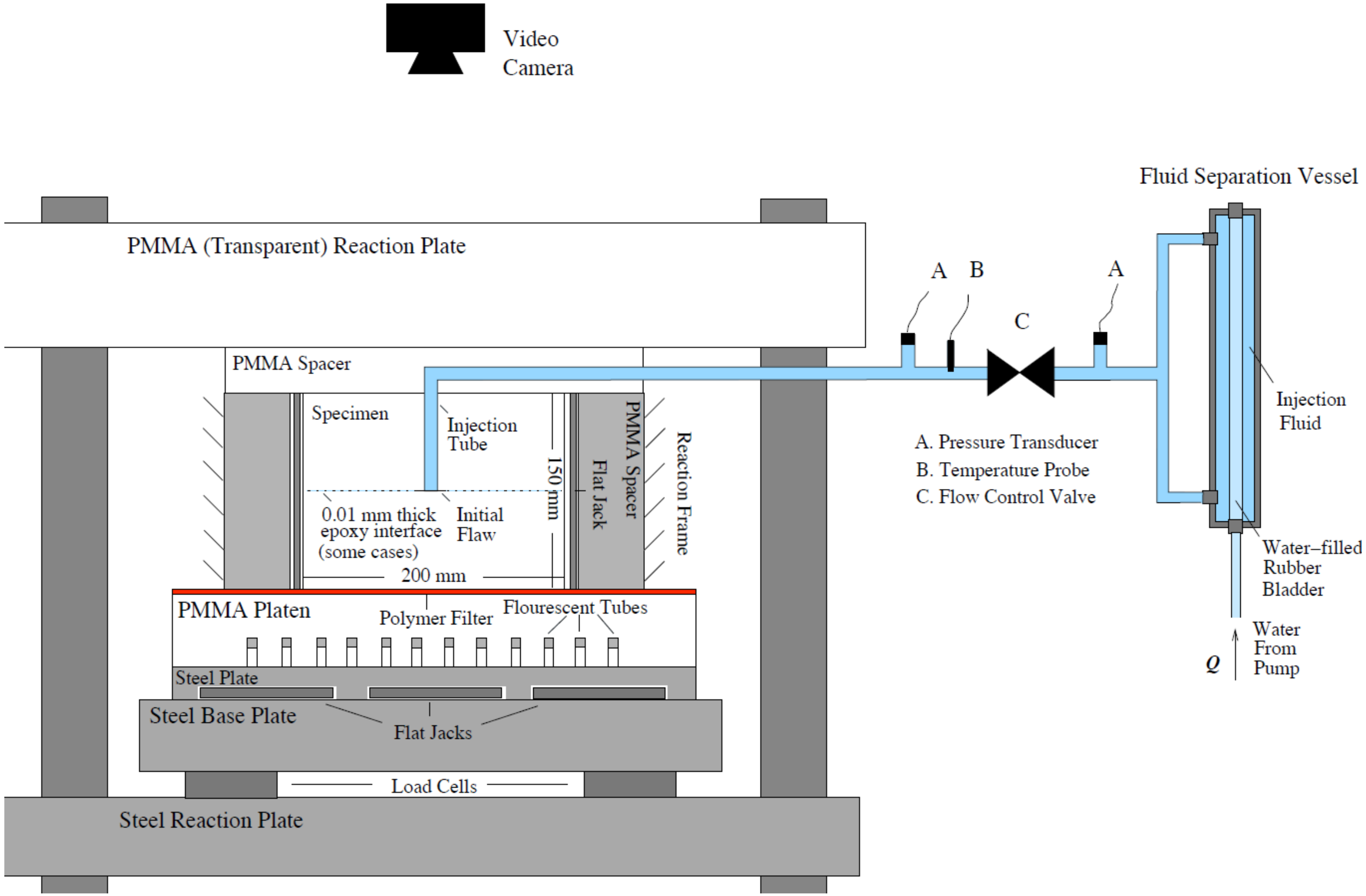

σ_o = "Overburden" stress

v_{tip} = Tip velocity

μ' = Dynamic fluid viscosity $* \, 12$

E' = Plane strain modulus

K' = Fracture Toughness $* \, (32/\pi)^{1/2}$

Particular Case: Zero Lag

$$\kappa = \left(\frac{\sigma_o K'^2}{\mu' v_{tip} E'^2} \right)^{1/2} \geq 1$$

Bunger AP, Detournay E. 2008. J Mech Phys Solids, 56(11):3101-3115.

Experiment in Progress

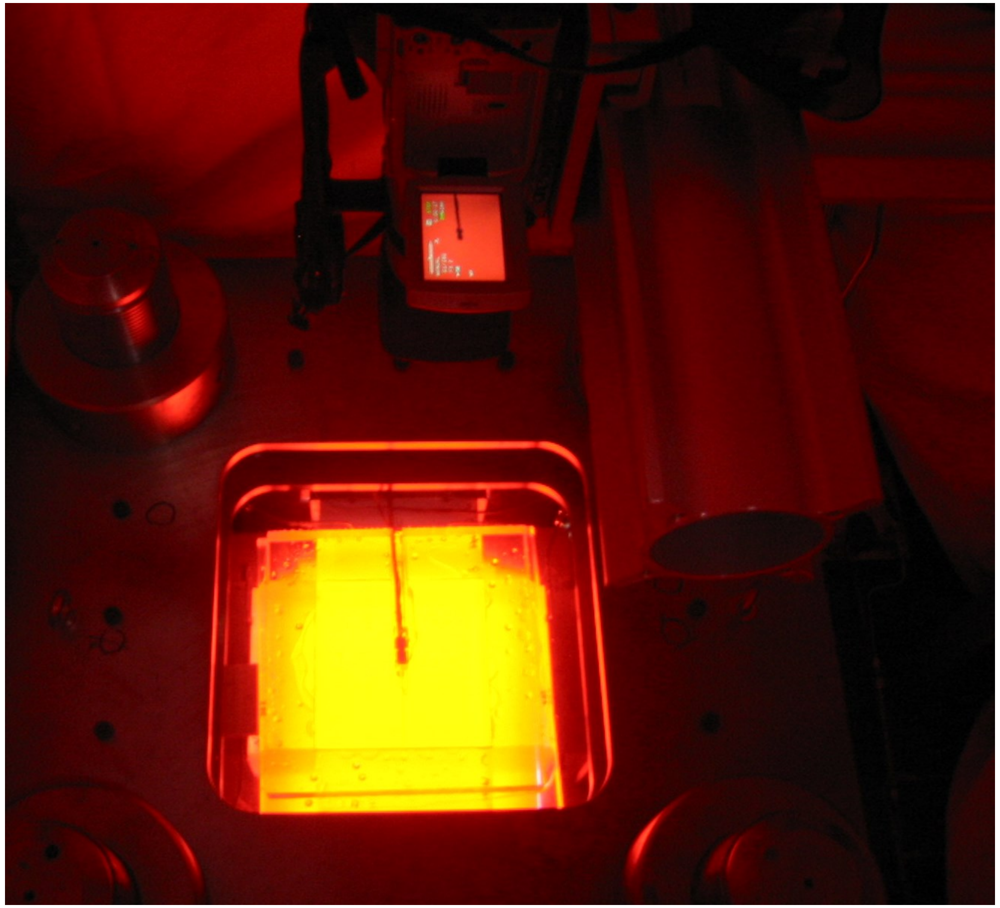

Toughness-dominated Example

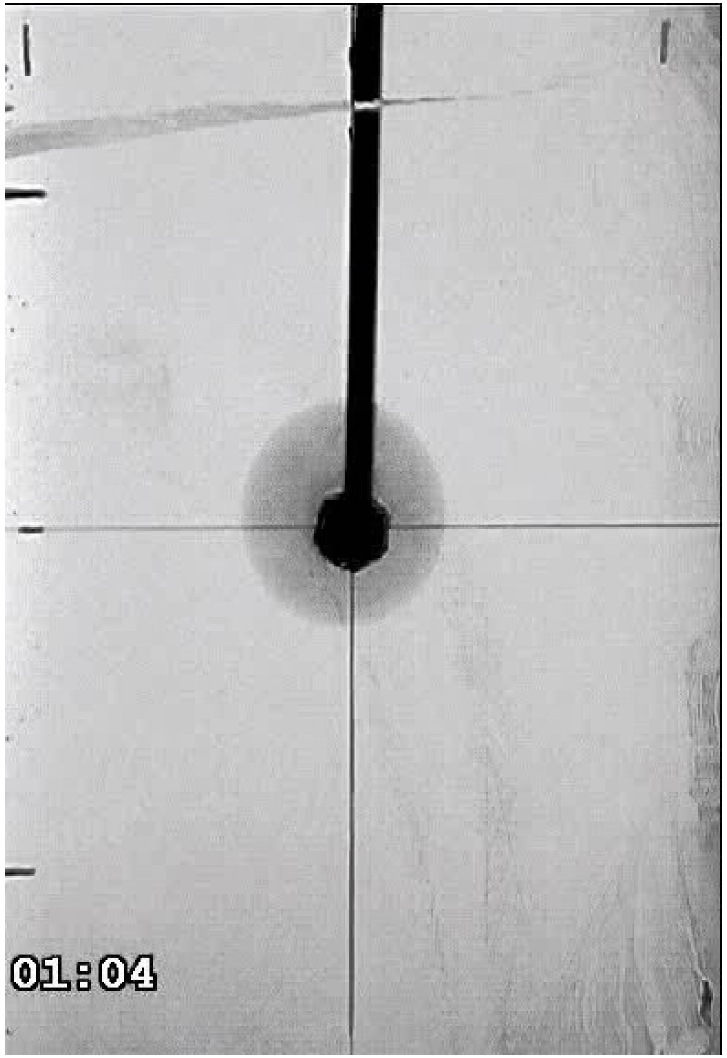

Viscosity-dominated Example

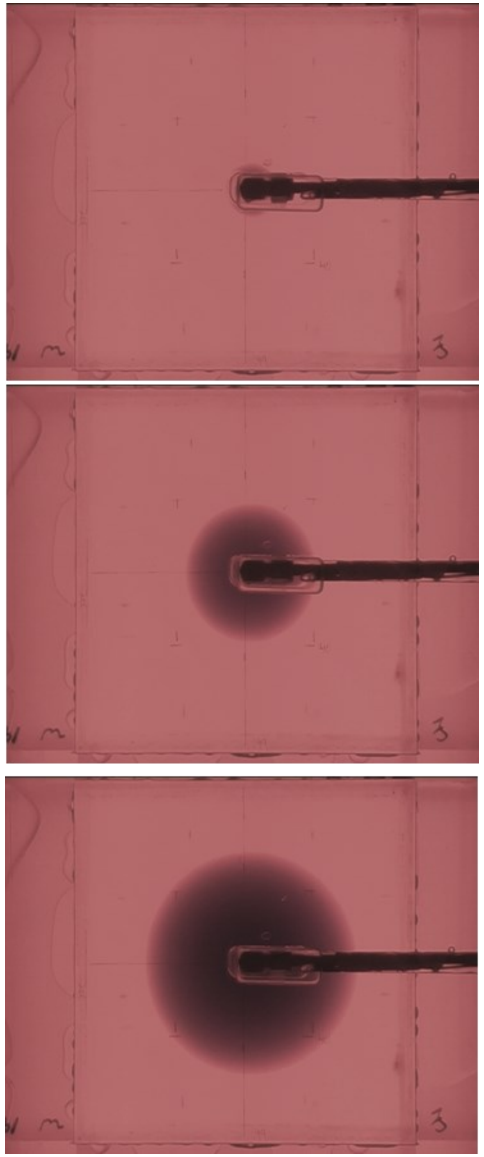

For predictions of symmetry breaking see: Gao, H., & Rice, J. R. (1987). Somewhat circular tensile cracks. *International Journal of Fracture*, *33*(3), 155-174.

Photometric Analysis

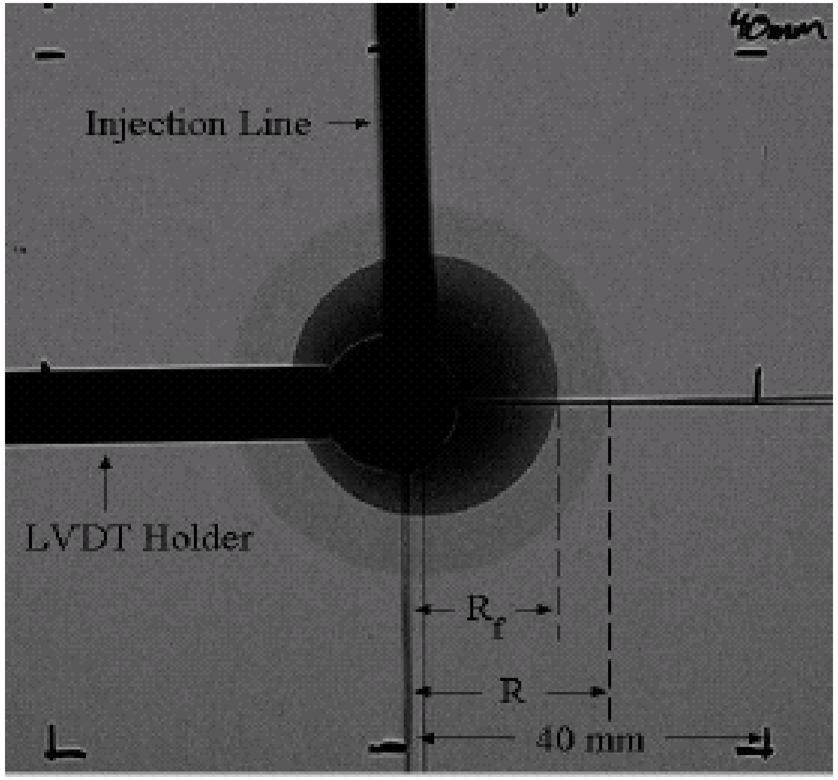

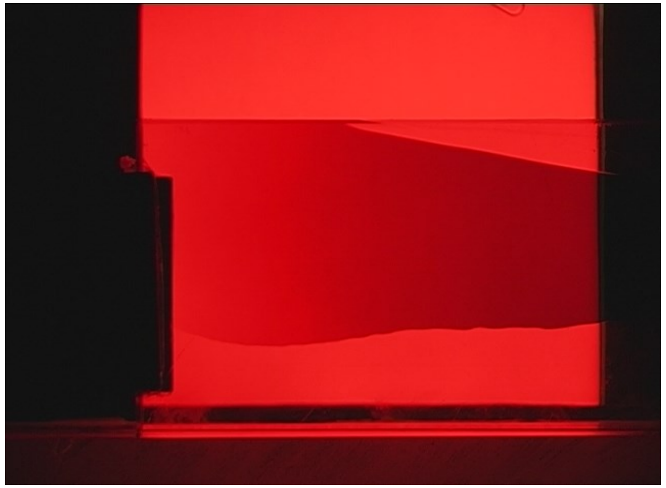

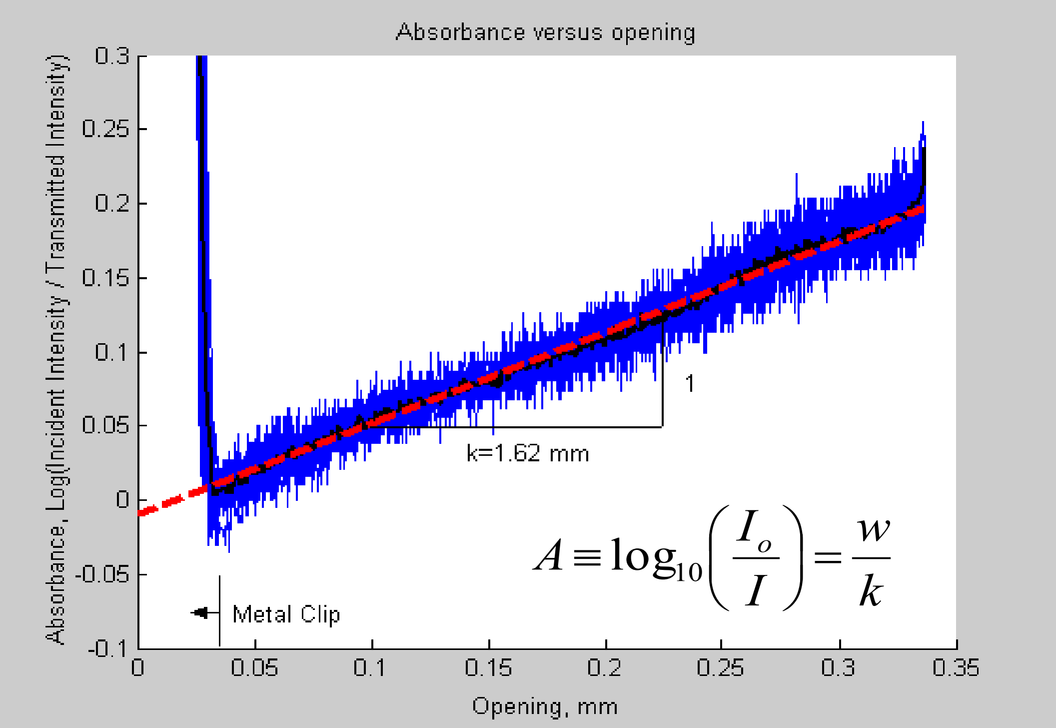

Bunger, Meas. Sci. Technol., 17:3237-3244, 2006

Near-Tip Behavior Following LEFM

Linear Elastic Fracture Mechanics

$$w \sim 4\left(\frac{2}{\pi}\right)^{1/2} \frac{K_{Ic}}{E'} s^{1/2}$$

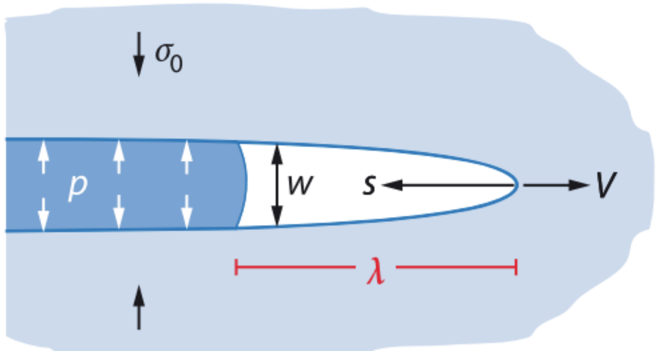

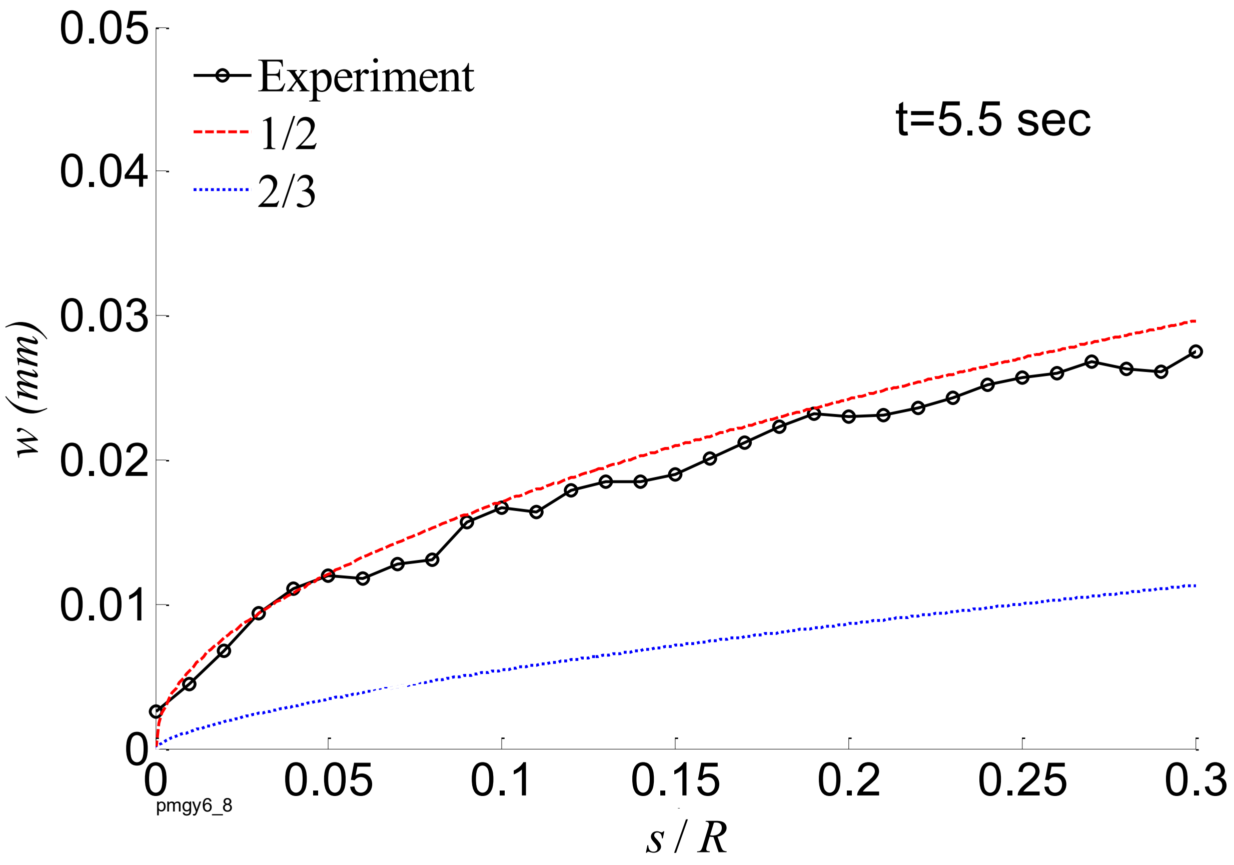

Material: PMMA
Viscosity=0.1 Pa s
"Toughness Regime"

Bunger AP, Detournay E. 2008. J Mech Phys Solids, 56(11):3101-3115.

Near-Tip Behavior Deviating from LEFM

Fluid/Solid Coupling in Tip Region

$$w \sim 2 \cdot 3^{7/6} \left(\frac{\mu v_{tip}}{E'} \right)^{1/3} s^{2/3}$$

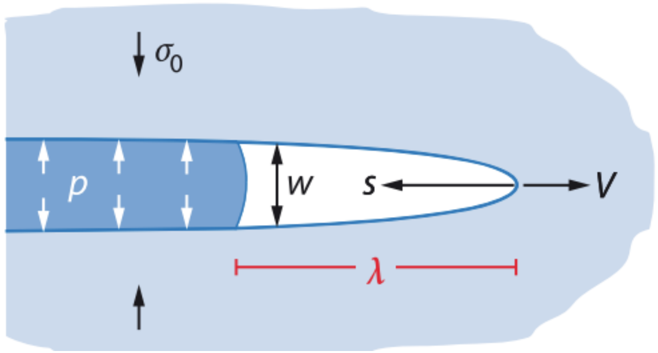

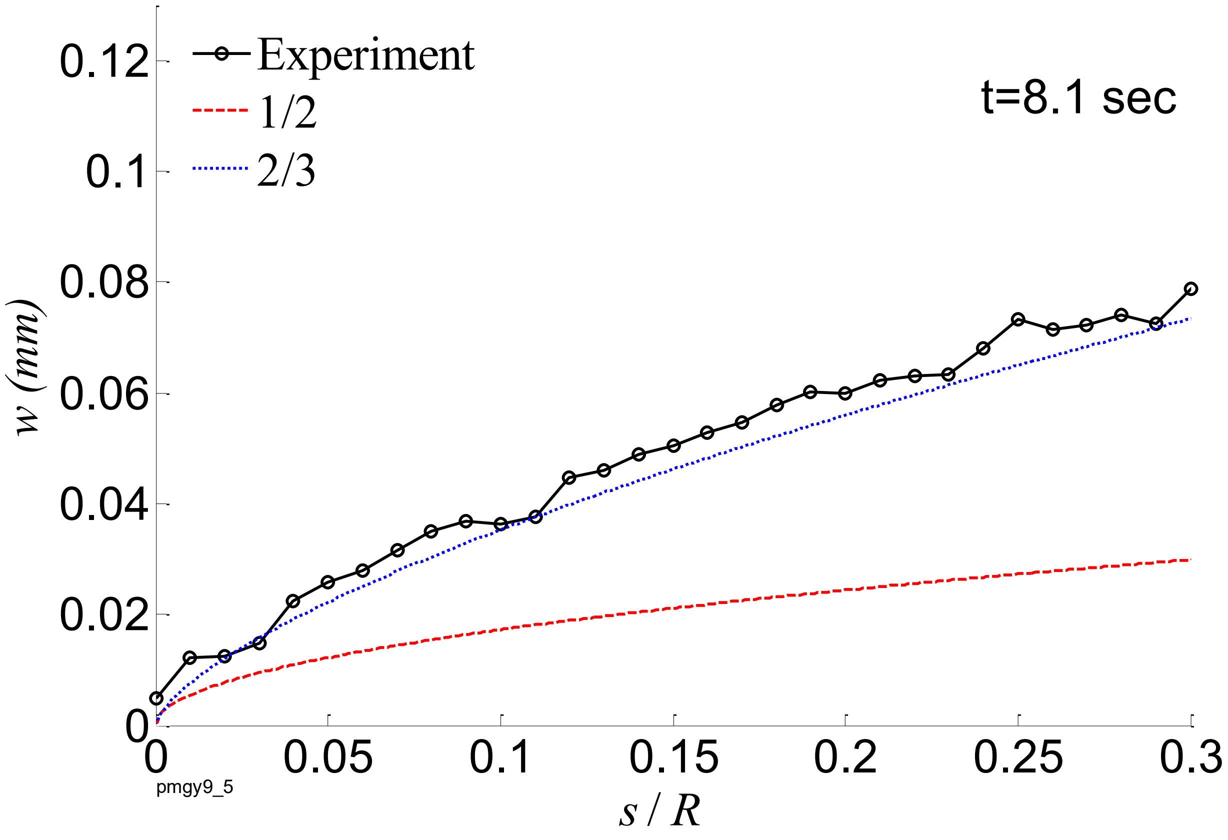

Material: PMMA
Viscosity=29 Pa s
"Viscosity Regime"

Garagash, D., & Detournay, E. (2000). *J. Appl. Mech. 67*(1), 183-192;
Garagash, D. I., & Detournay, E. (2005). *J. Appl. Mech. 72*(6), 916-928.

Bunger AP, Detournay E. 2008. J Mech Phys Solids, 56(11):3101-3115.

Implications of Fluid-Solid Coupling for Simulations

- Propagation implies LEFM width profile near tip
- But, elasticity and fluid flow near the tip brings in a different tip profile
- Each physical process brings its own characteristic length scale

Multiphysics problems are multiscale problems

- **In simulations leads to mesh dependence and very slow convergence with mesh refinement**

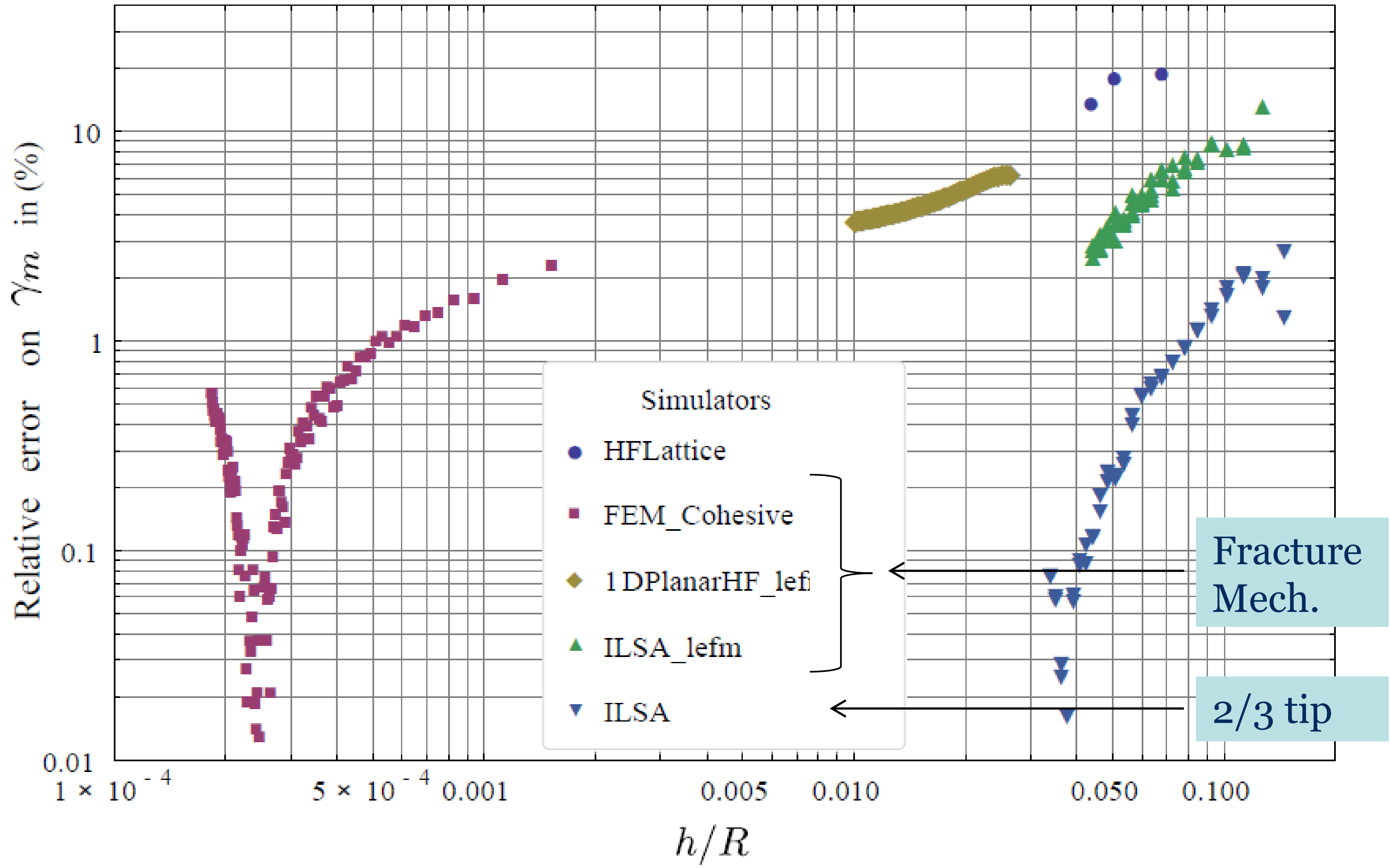

Lecampion et al. 2013. In: Effective and Sustainable Hydraulic Fracturing. ISBN 978-953-51-1137-5, (Intech), Chapter 43.

Homogeneous, transparent, brittle materials (PMMA, glass)

…to…

Actual rock

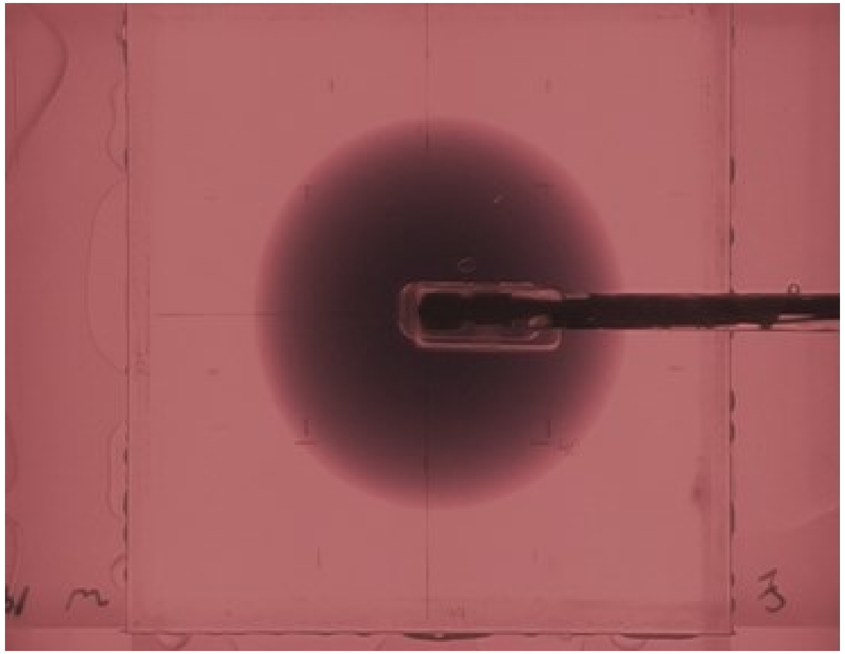

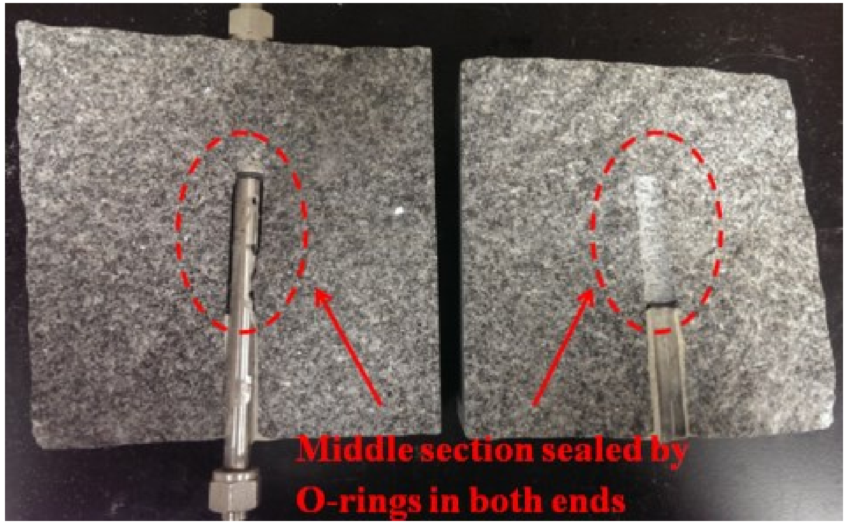

Lab Experiments – Time-Dependent Initiation

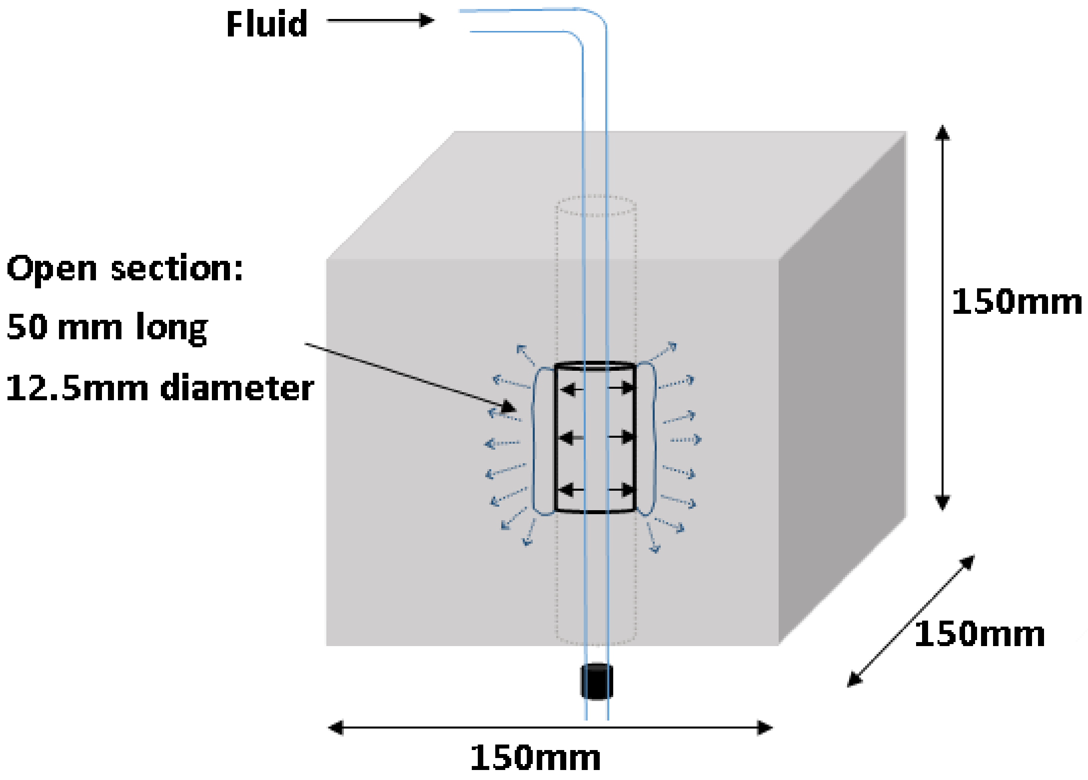

Before

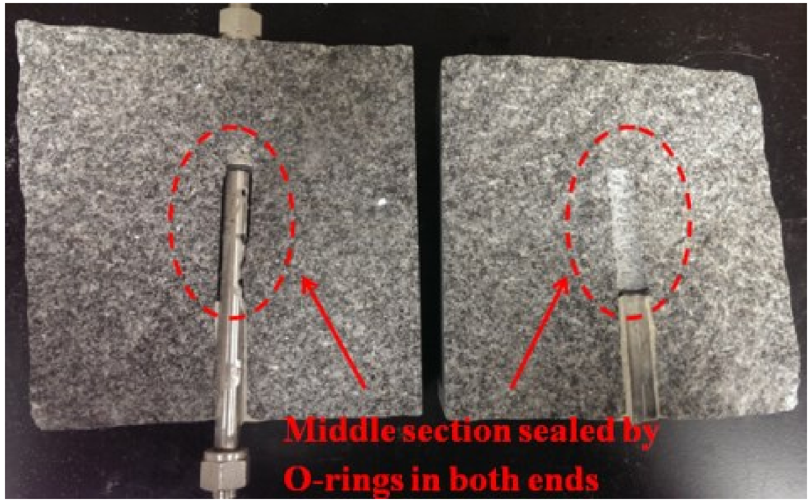

After

- Hold constant pressure
- Measure time to HF initiation

Lu G, Gordeliy E, Prioul R, Aidagulov G, Uwaifo EC, Ou Q, Bunger AP. 2020. Time Dependent Hydraulic Fracture Initiation. Journal of Geophysical Research – Solid Earth, 125, e2019JB018797.

Lab Experiments – Time-Dependent Initiation

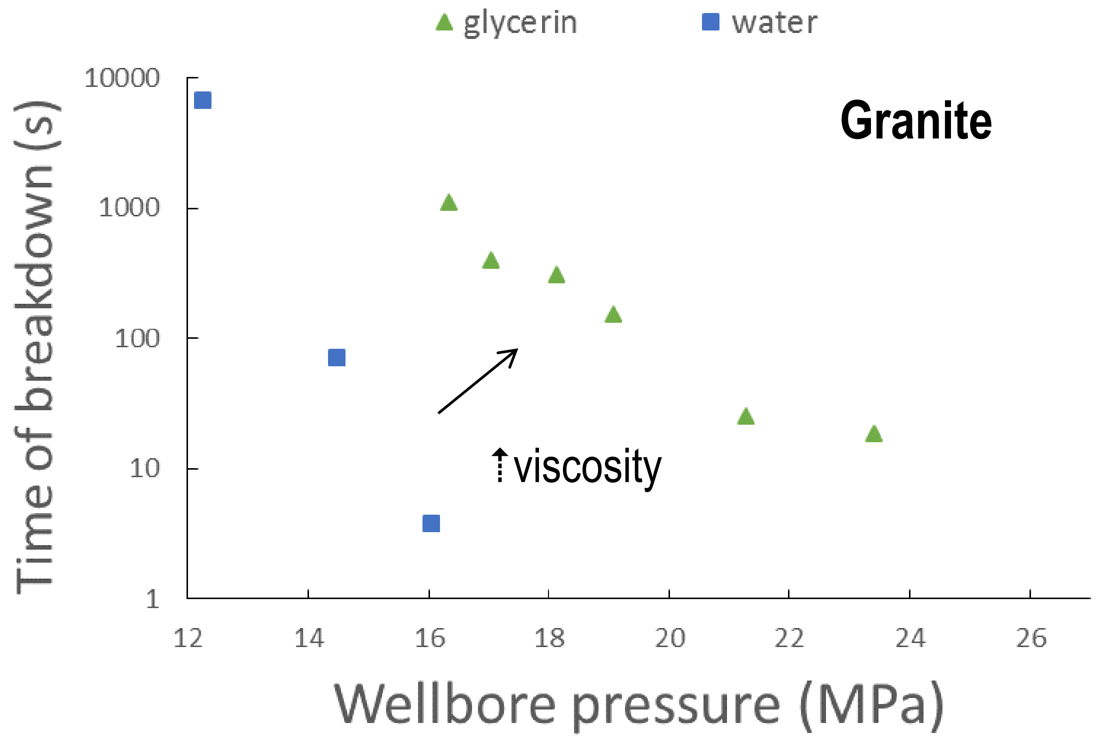

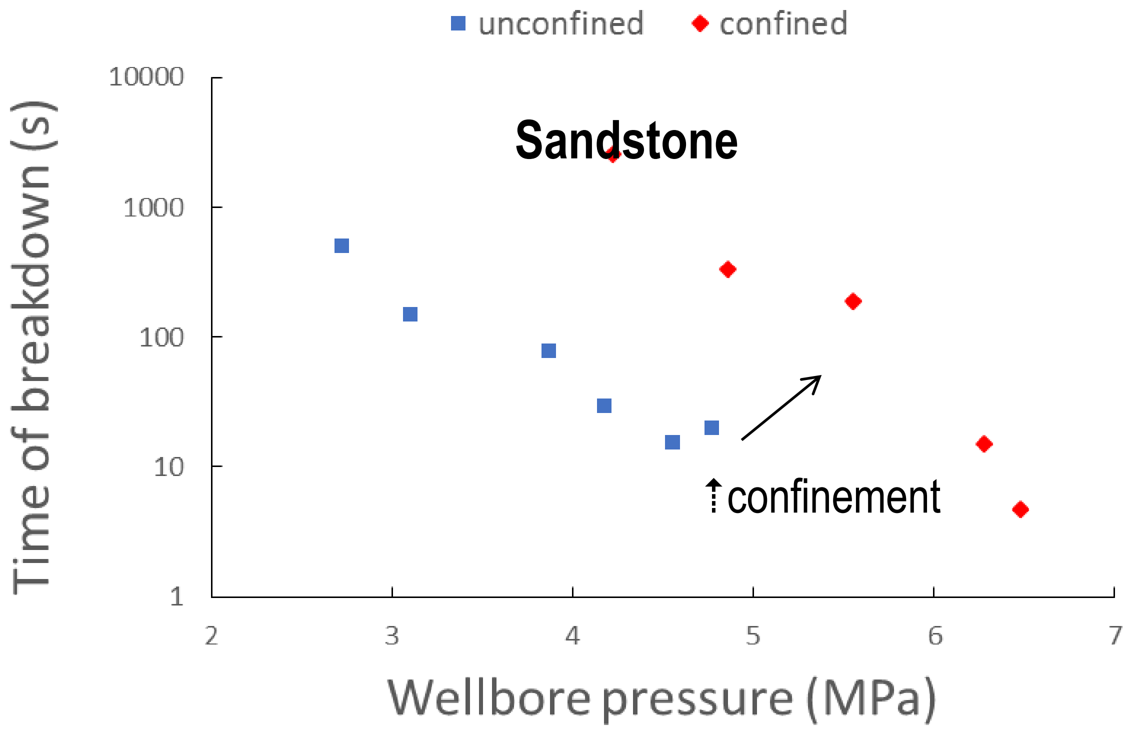

- Similar observation in both rock types
- Delay time increases with viscosity and confining stress

Lu G, Gordeliy E, Prioul R, Aidagulov G, Uwaifo EC, Ou Q, Bunger AP. 2020. Time Dependent Hydraulic Fracture Initiation. Journal of Geophysical Research – Solid Earth, 125, e2019JB018797.

Modeling Time-Dependent Initiation

- Classical hydraulic fracture model but changing propagation velocity to Charles' law for subcritical crack growth

$$V = A\left(\frac{K_{\mathrm{I}}}{K_{\mathrm{IC}}}\right)^n,$$

- With some algebra, tip condition becomes

$$w \sim \sqrt{\frac{32}{\pi}}\frac{K_{\mathrm{IC}}}{E'}(x_{tip}-x)^{1/2}\cdot\left(\frac{V}{A}\right)^{1/n},\ x \to x_{tip}$$

- Good match to experiments, using exponent *n* as a fitting parameter (noting *n* is in reasonable ranges for these two rocks)

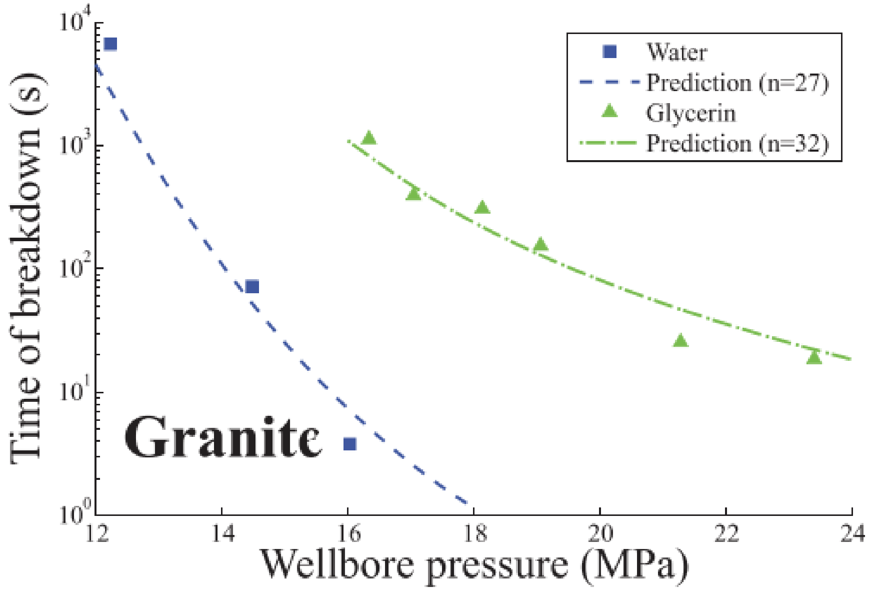

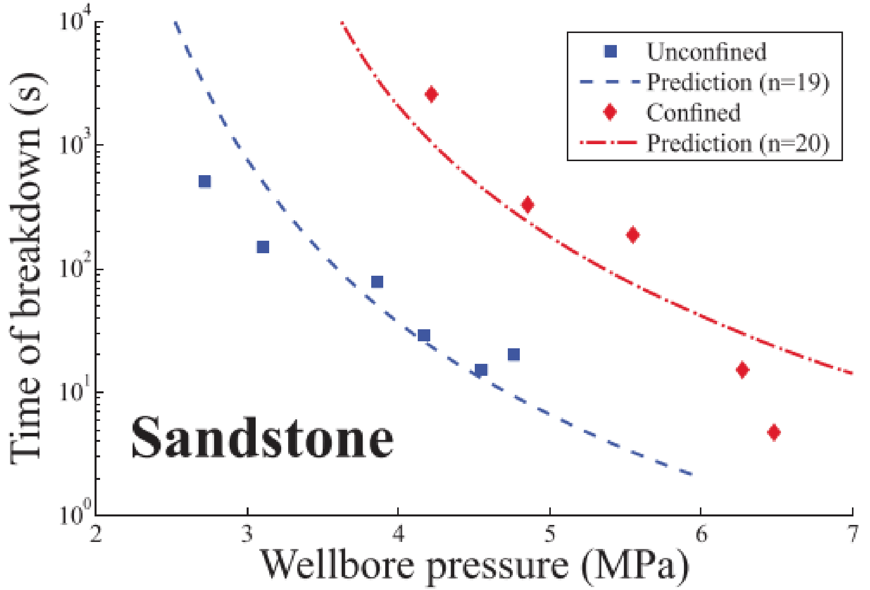

Lu G, Gordeliy E, Prioul R, Aidagulov G, Uwaifo EC, Ou Q, Bunger AP. 2020. Time Dependent Hydraulic Fracture Initiation. Journal of Geophysical Research – Solid Earth, 125, e2019JB018797.

Acoustic Emission during Time Dependent Breakage of Rocks

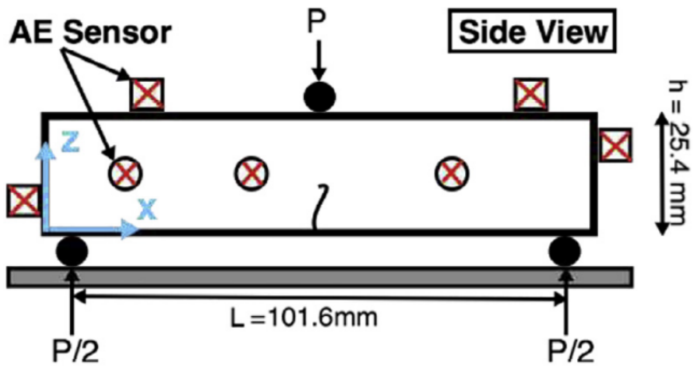

- Hold constant load
- Measure acoustic emission until time of failure

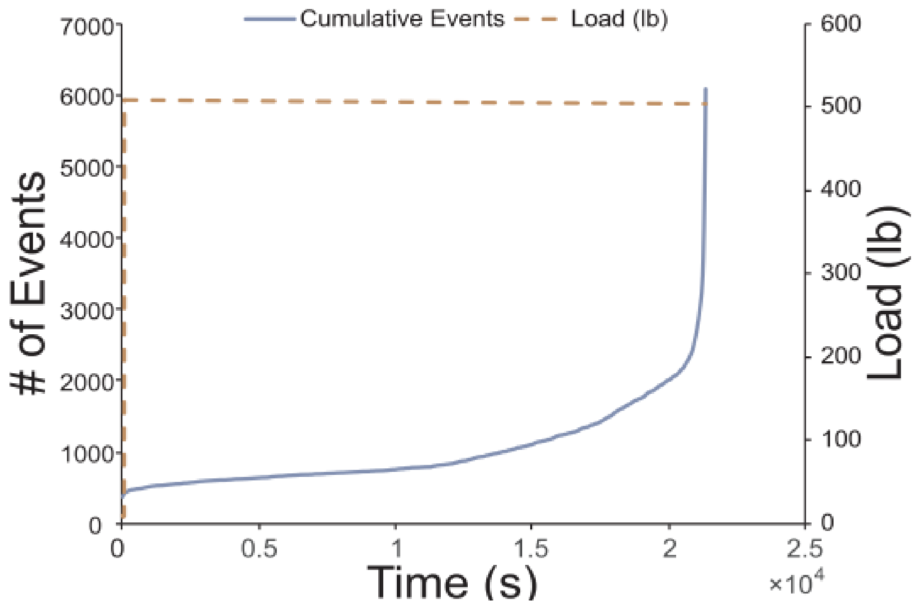

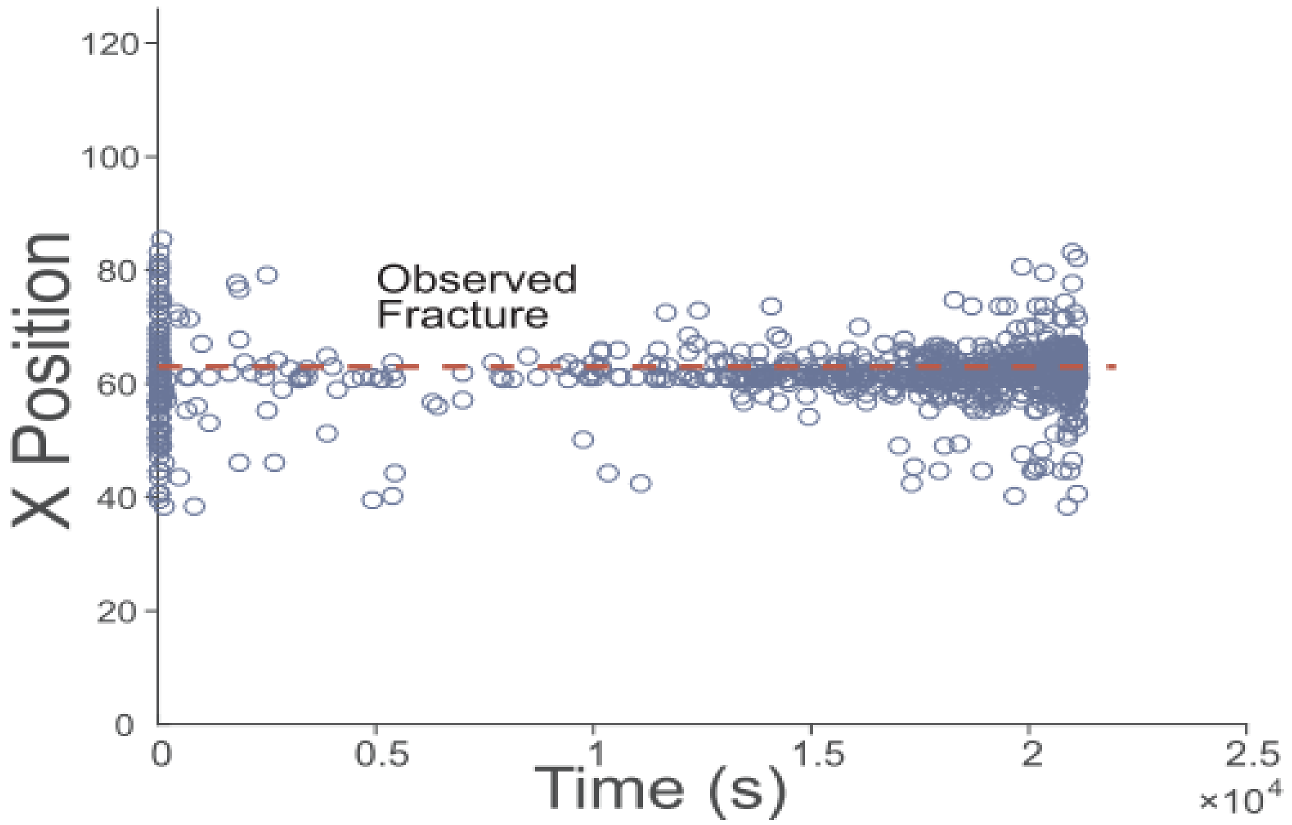

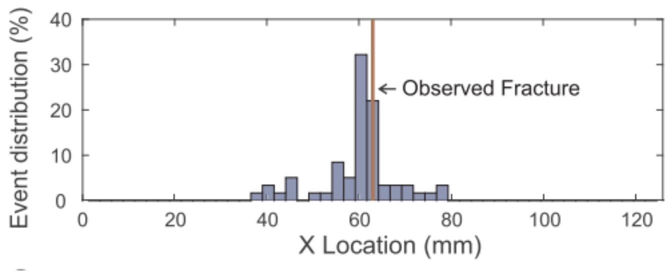

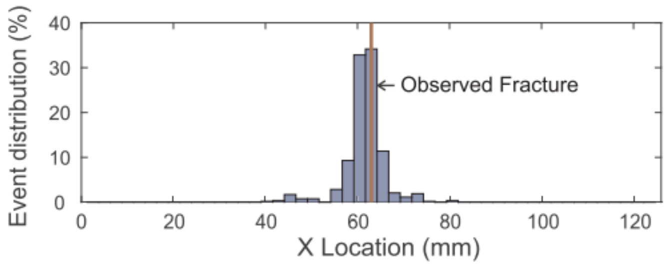

Winner, R. A., Lu, G., Prioul, R., Aidagulov, G., & Bunger, A. P. (2018). Acoustic emission and kinetic fracture theory for time-dependent breakage of granite. *Engineering Fracture Mechanics*, *199*, 101-113.

Acoustic Emission during Time Dependent Breakage of Rocks

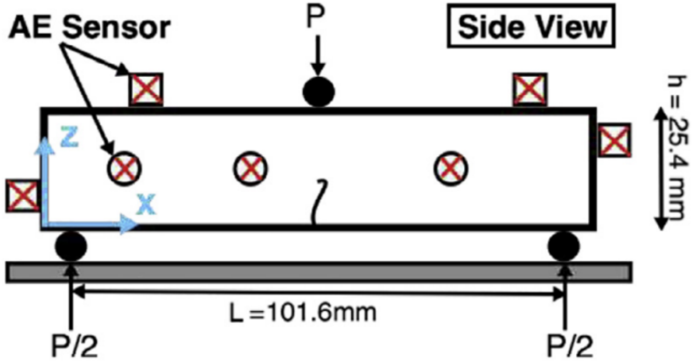

- Hold constant load
- Measure acoustic emission until time of failure

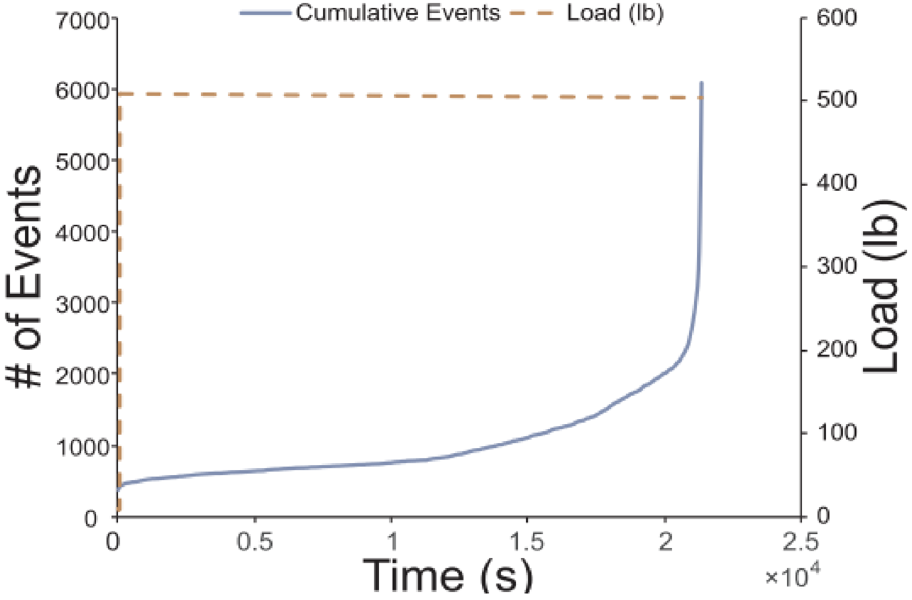

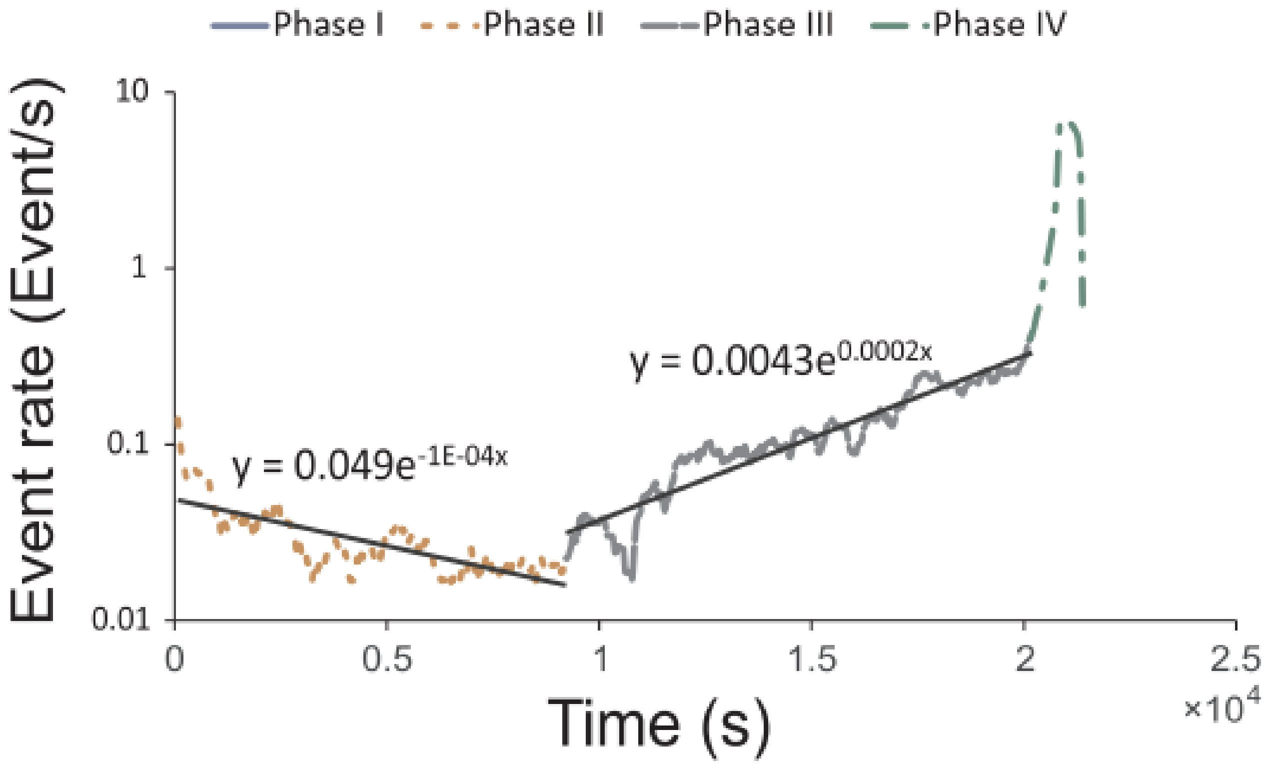

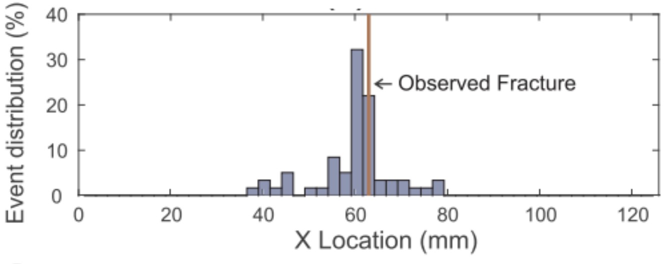

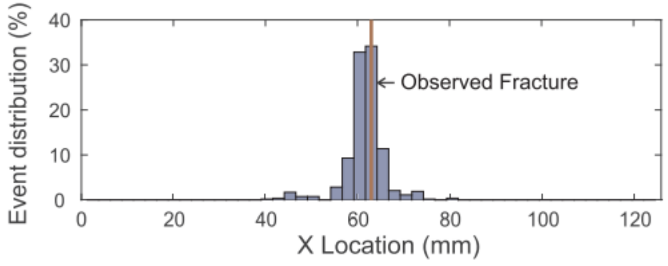

Winner, R. A., Lu, G., Prioul, R., Aidagulov, G., & Bunger, A. P. (2018). Acoustic emission and kinetic fracture theory for time-dependent breakage of granite. *Engineering Fracture Mechanics*, *199*, 101-113.

Acoustic Emission during Time Dependent Breakage of Rocks

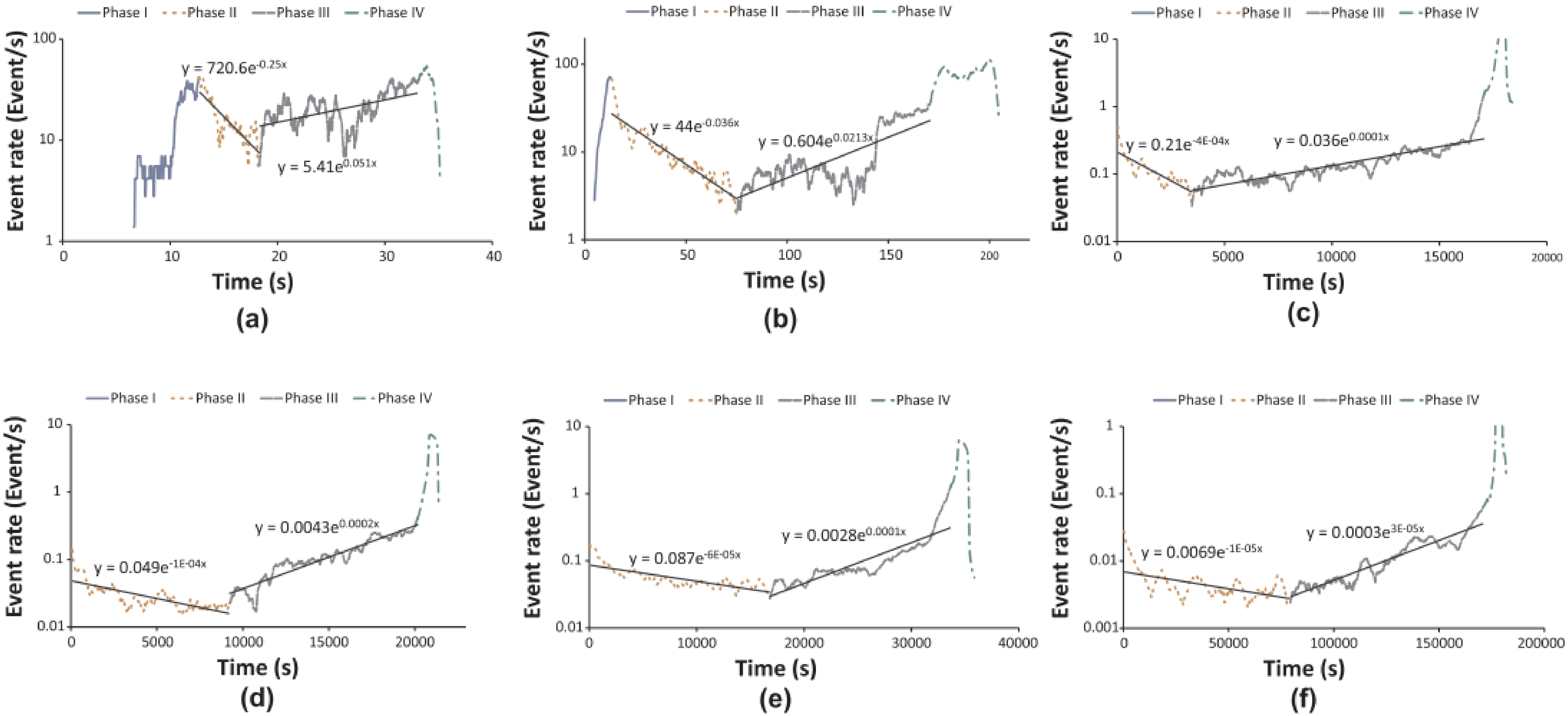

- Range of lifetimes: O(10^1)-O(10^5) seconds
- All cases, transition from declining to increasing event rate occurs just before halfway to breakage

Winner, R. A., Lu, G., Prioul, R., Aidagulov, G., & Bunger, A. P. (2018). Acoustic emission and kinetic fracture theory for time-dependent breakage of granite. *Engineering Fracture Mechanics*, *199*, 101-113.

Acoustic Emission Aftershocks

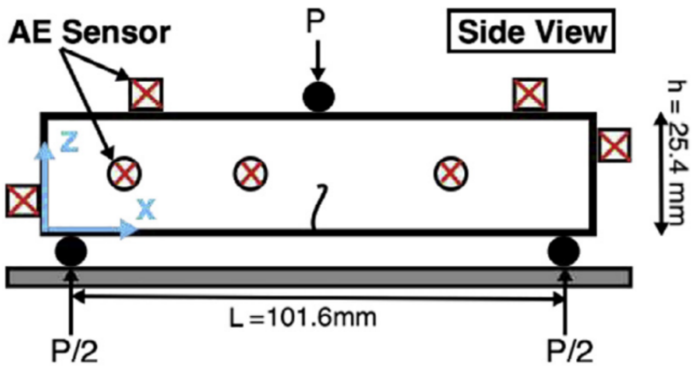

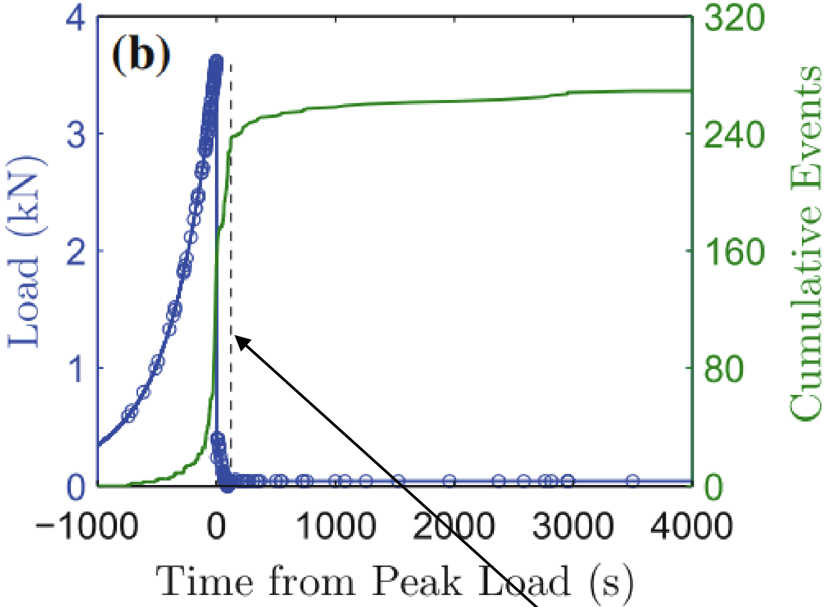

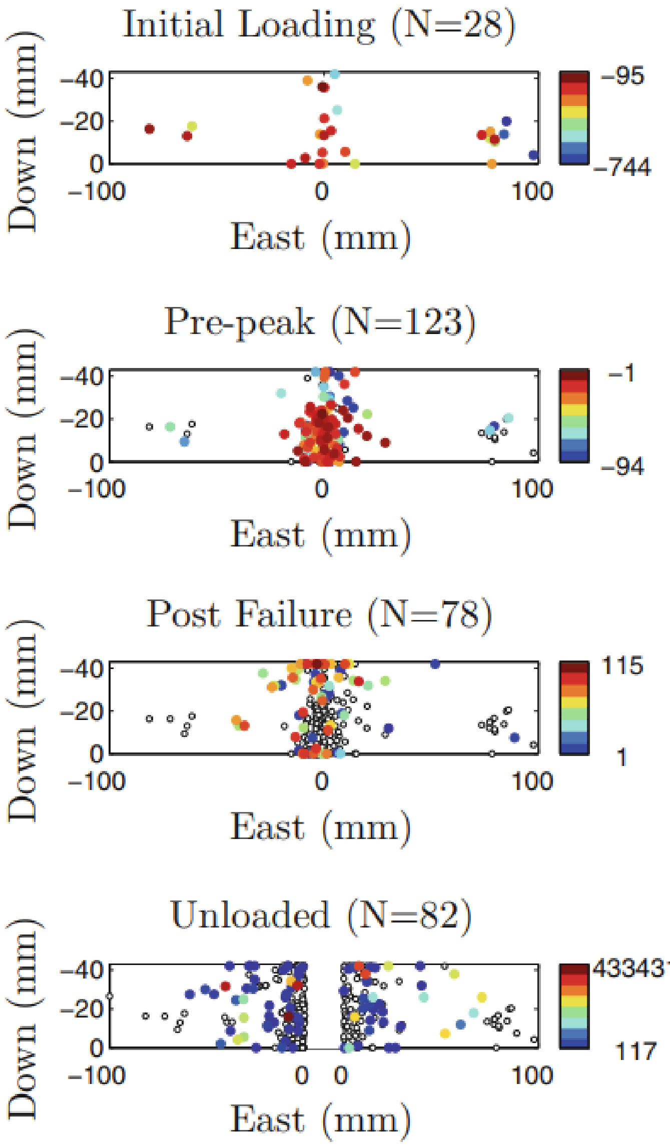

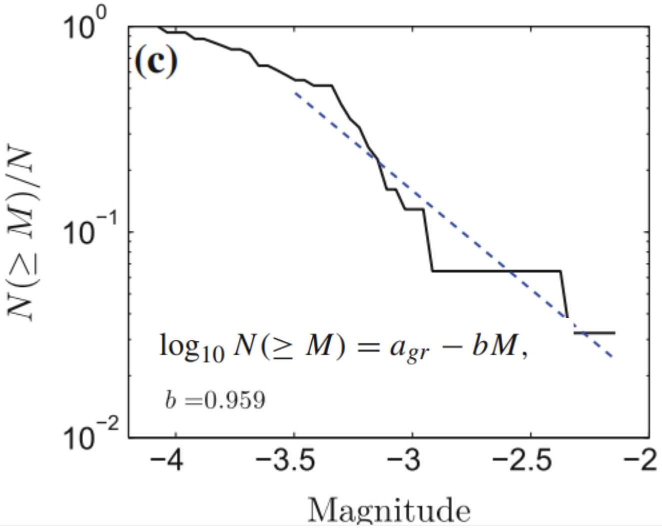

Magnitudes follow Gutenberg-Richter law

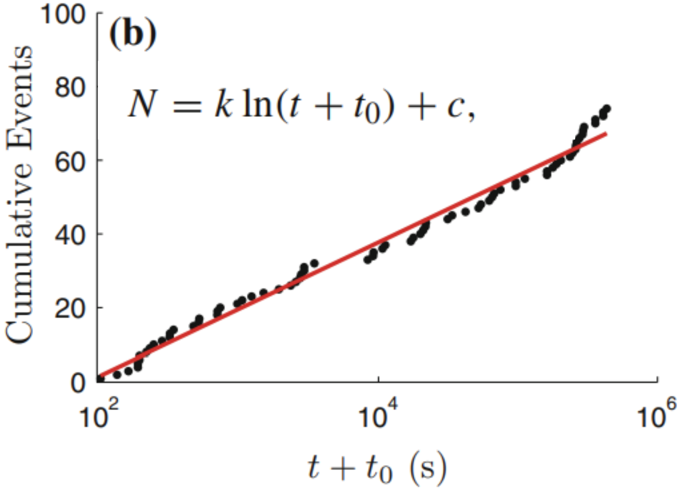

Frequency follows Omori-Utsu law

- Increase load to failure
- Separate halves, isolate on rubber mats
- Observe events continuing for hours to days after breakage

Bunger, A. P., Kear, J., Dyskin, A. V., & Pasternak, E. (2015). Sustained acoustic emissions following tensile crack propagation in a crystalline rock. *International Journal of Fracture*, *193*(1), 87-98.

Laboratory scale

…to…

Field scale

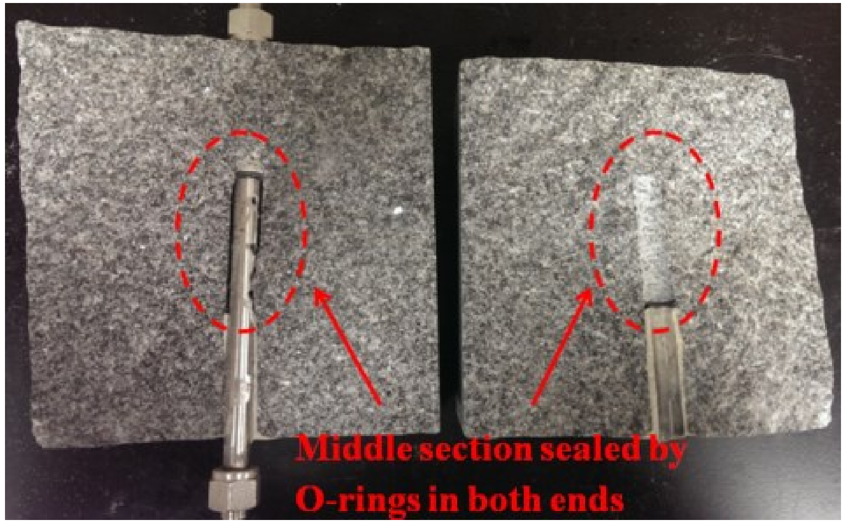

Subsurface Pumped Energy Storage

- Create a storage lens by pumping viscous fluid into the subsurface
- Energy storage: Inflate lens by pumping water during high power production times (i.e. daytime)
- Energy production: Produce water from lens during low production times to drive a turbine (i.e. evening/night)
- Pressure and flowing rate in proportion to the difference between rock density and fluid density

"Virtual Reality," by Christoph Niemann.

Reporting

ANNALS OF INNOVATION

THE RENEWABLE-ENERGY REVOLUTION WILL NEED RENEWABLE STORAGE

Can gravity, pressure, and other elemental forces save us from becoming a battery-powered civilization?

By Matthew Hutson

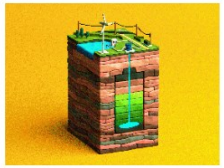

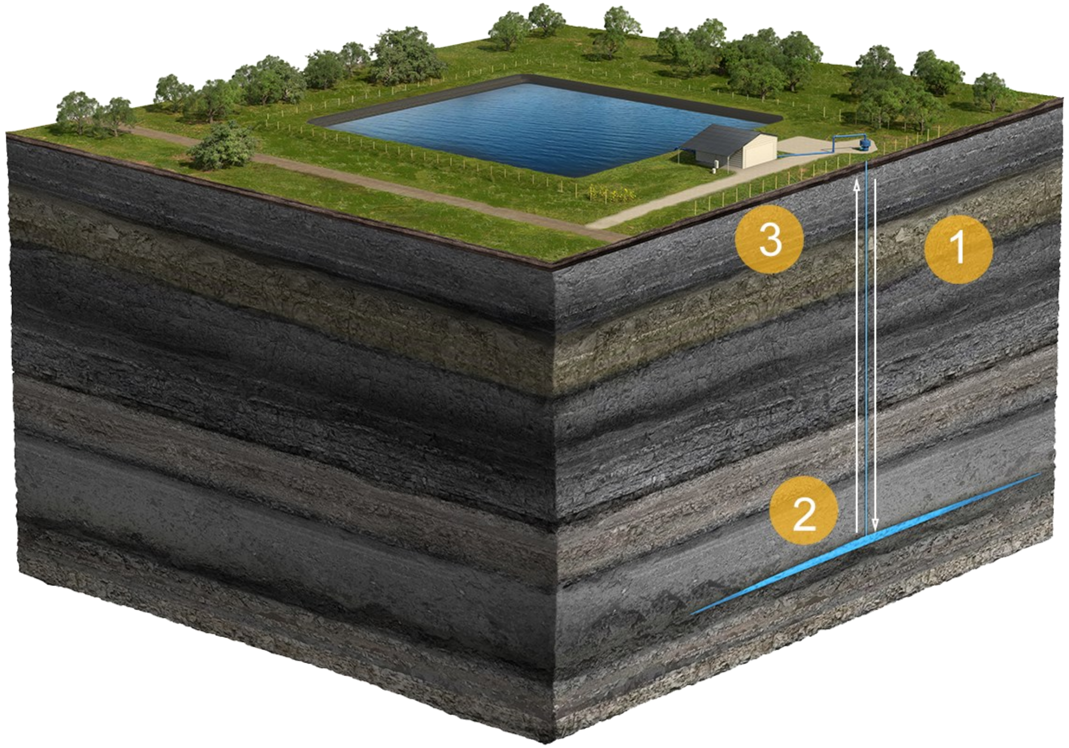

https://www.newyorker.com/magazine, April 25 and May 2, 2022 Issue

https://quidnetenergy.com/solution/?section=technologySection

LOBSTER Governing Equations

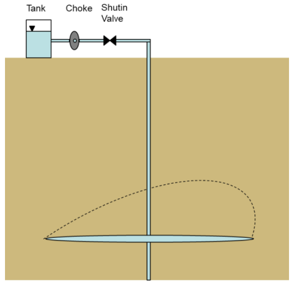

Similar to classical hydraulic fracture model

- Elasticity, solved by Displacement Discontinuity Method (elastic half space, circular, horizontal, planar crack) with addition of bridge stress

$$p_{f,i} - \sigma_o = -\frac{E'}{R}\sum_{j=1}^{m} A_{ij} w_j - s_i(w_i)$$

- Continuity Equation including matrix and pressure dependent fissure leakoff (local fluid mass balance, solved by finite difference method)

$$\frac{\partial w}{\partial t} + \frac{1}{r}\frac{\partial}{\partial r}(rq) + 2v_{\ell,mf} = 0, \qquad q = \langle v \rangle w$$

- Fluid flux equation valid for all Reynold's numbers

$$q = -\frac{w^3}{12\mu \bar{f}_D(Re,\upsilon)}\frac{\partial p_f}{\partial r}$$

- Tip Boundary Conditions

$$w(R,t) = 0, \quad q(R,t) = 0$$

Unique to pumped subsurface storage

- Mixed inlet boundary condition (choke coupling wellhead pressure to flowing rate, can obtain this via classical energy equation from Fluid Mechanics)

$$Q_{BH} = F\left(d_o, f_g, \rho_f, H, h_s, p_{net}\right)$$

$$\lim_{r \to R_w} 2\pi r q = -Q_{BH}$$

Also can switch inlet condition to injection to simulate reinflation of existing lens

w=width
p_f=fluid pressure
q=fluid flux
Q_{BH}=volumetric outflow rate
f_g=stress gradient
H=depth
R=radius
μ=fluid viscosity
E'=plane strain modulus
ρ_f=fluid density
d_o=choke aperture
C_d=choke shape factor
p_{net}=p_f-$f_g H$
p'=f_g-$\rho_f g$

Behavior of a Lens when Emptied to the Point of Pinching

- Initial quasi-steady flow rate and WH pressure (hence also power)
- Gives way at large time to rapid decline – "Pinching"
- Avoid by keeping sufficient surplus volume and designing flowback rate to be small enough

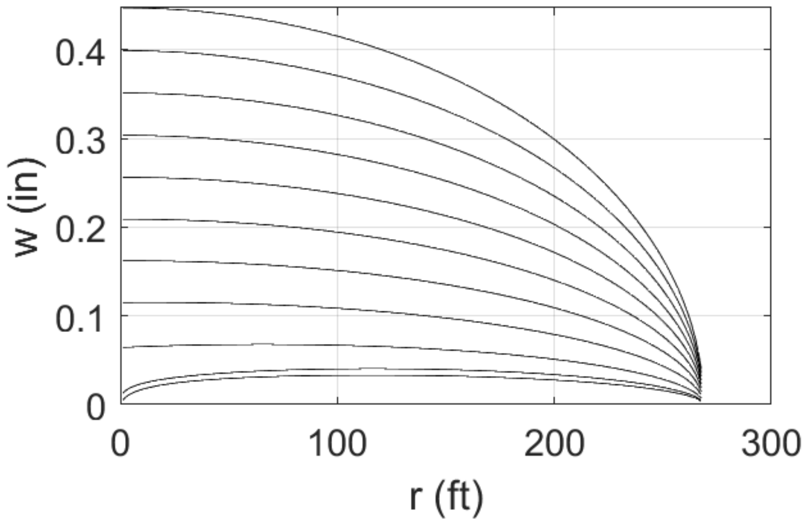

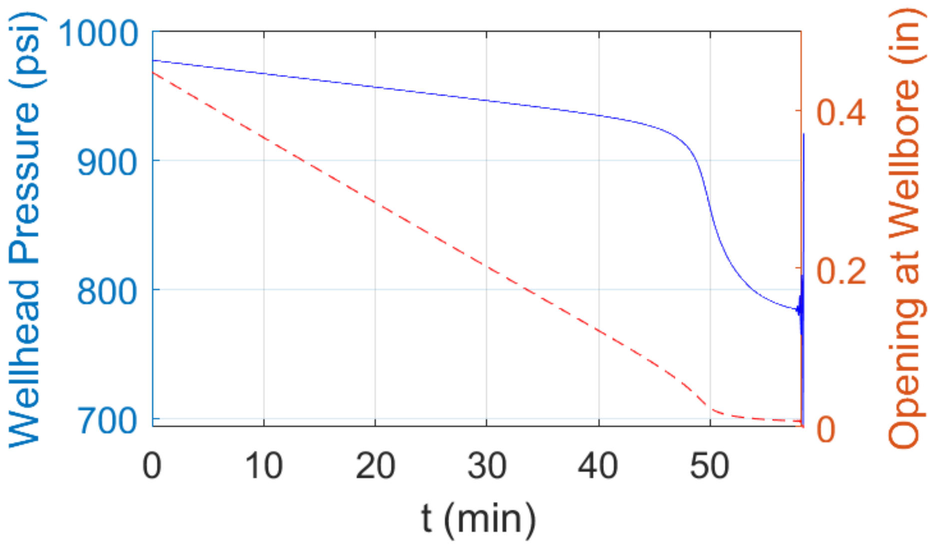

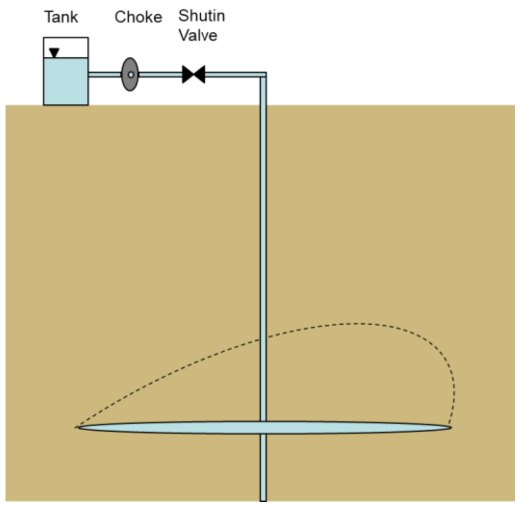

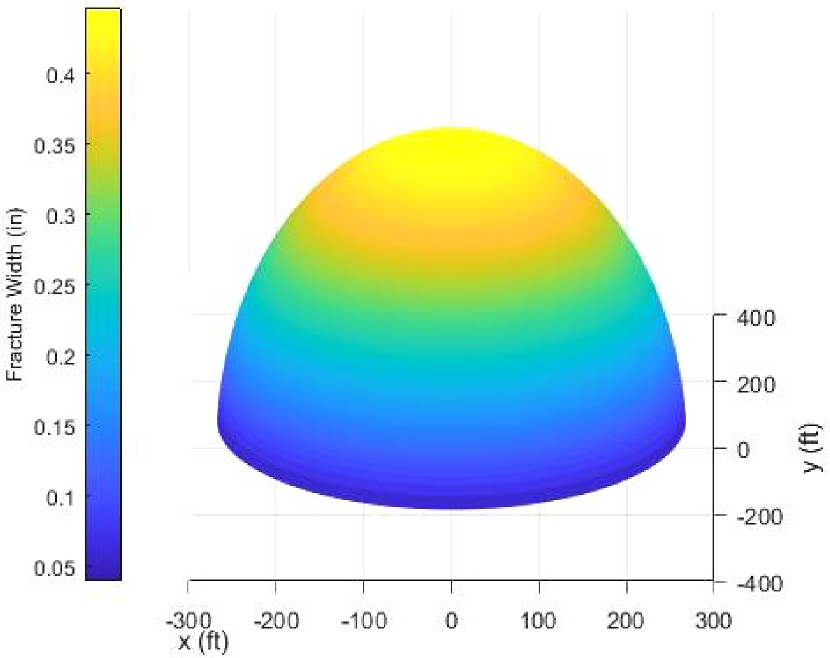

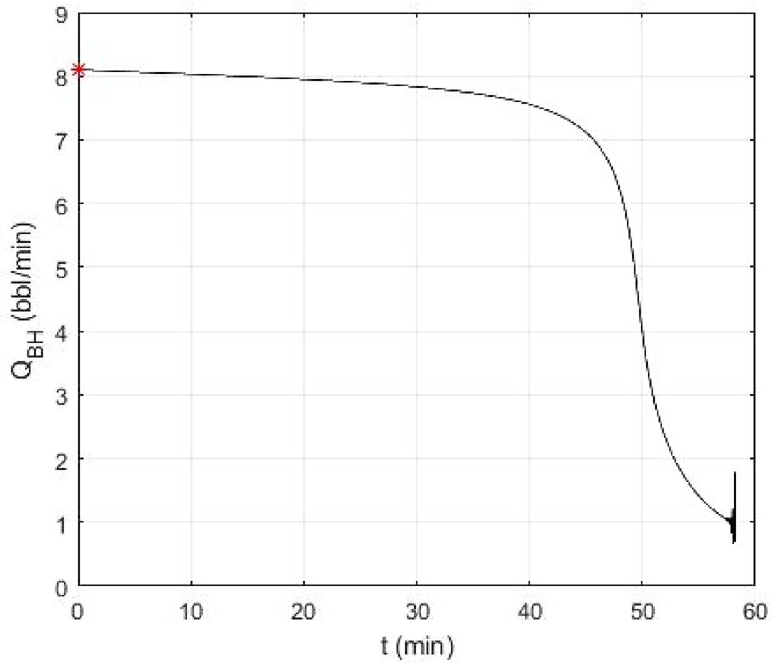

Example: 92% Efficiency, 40 kWh Design

- 40 kW, 60 minute flowback, 1378 ft depth with fg=1.07psi/ft and 0.4” choke
- **R=200m, Vi=800bbl, Qinj=2bbl/min**
- Pressure dependent leakoff with critical pressure at 1.13 psi/ft
- Cycles 160bbl, 5bbl loss per cycle (**97% fluid efficiency**)
- Returns 42.5 kWh energy from 46 kWh input (**92% RTE**)

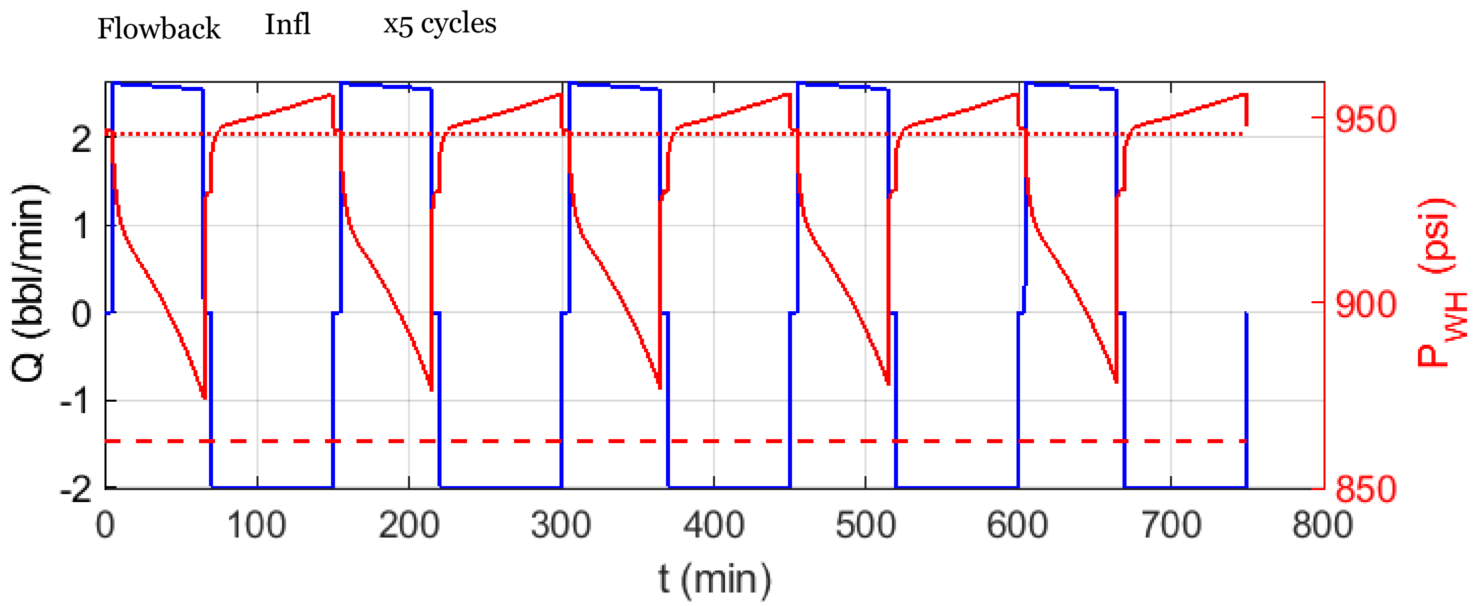

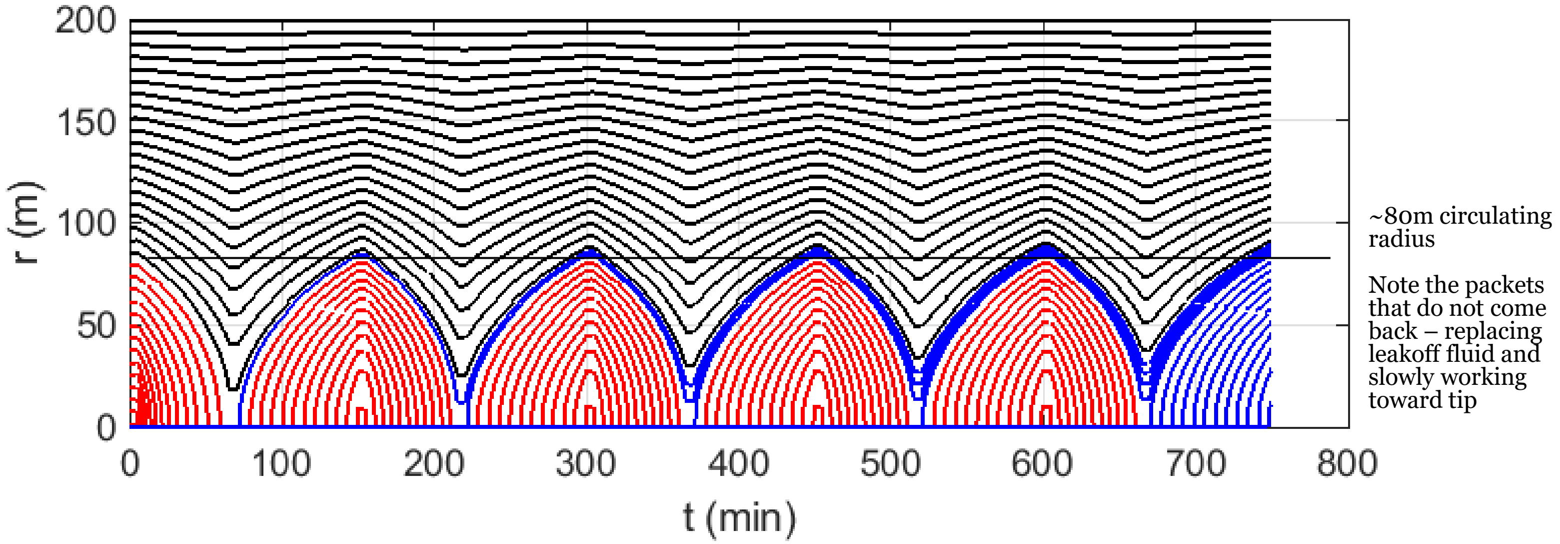

Packets starting in and staying in lens

Packets injected to and staying in lens

Packets produced out of the lens

Normalization of Compliance by (Full-Space) Elastic Solution

Volume and width from LEFM:

$$V_{lens} = \frac{16 p_{net} R^3}{3E'}, \qquad w_o = \frac{8 p_{net} R}{\pi E'}$$

Elastic Compliance:

$$\Rightarrow \frac{w_o}{p_{net}} = \frac{2^{5/3} 3^{1/3}}{\pi} \frac{V_{lens}^{1/3}}{E'^{2/3} p_{net}^{1/3}}$$

Divide compliance by elastic solution:

$$let: V_{lens} = \eta V_{inj}, \quad E'_{app} = B E'_{meas}$$

$$\chi = \frac{w_o}{\eta^{1/3} V_{inj}^{1/3}} \frac{E'^{2/3}}{p_{net}^{2/3}} \frac{\pi}{2^{5/3} 3^{1/3}} = \frac{1}{B^{2/3}}$$

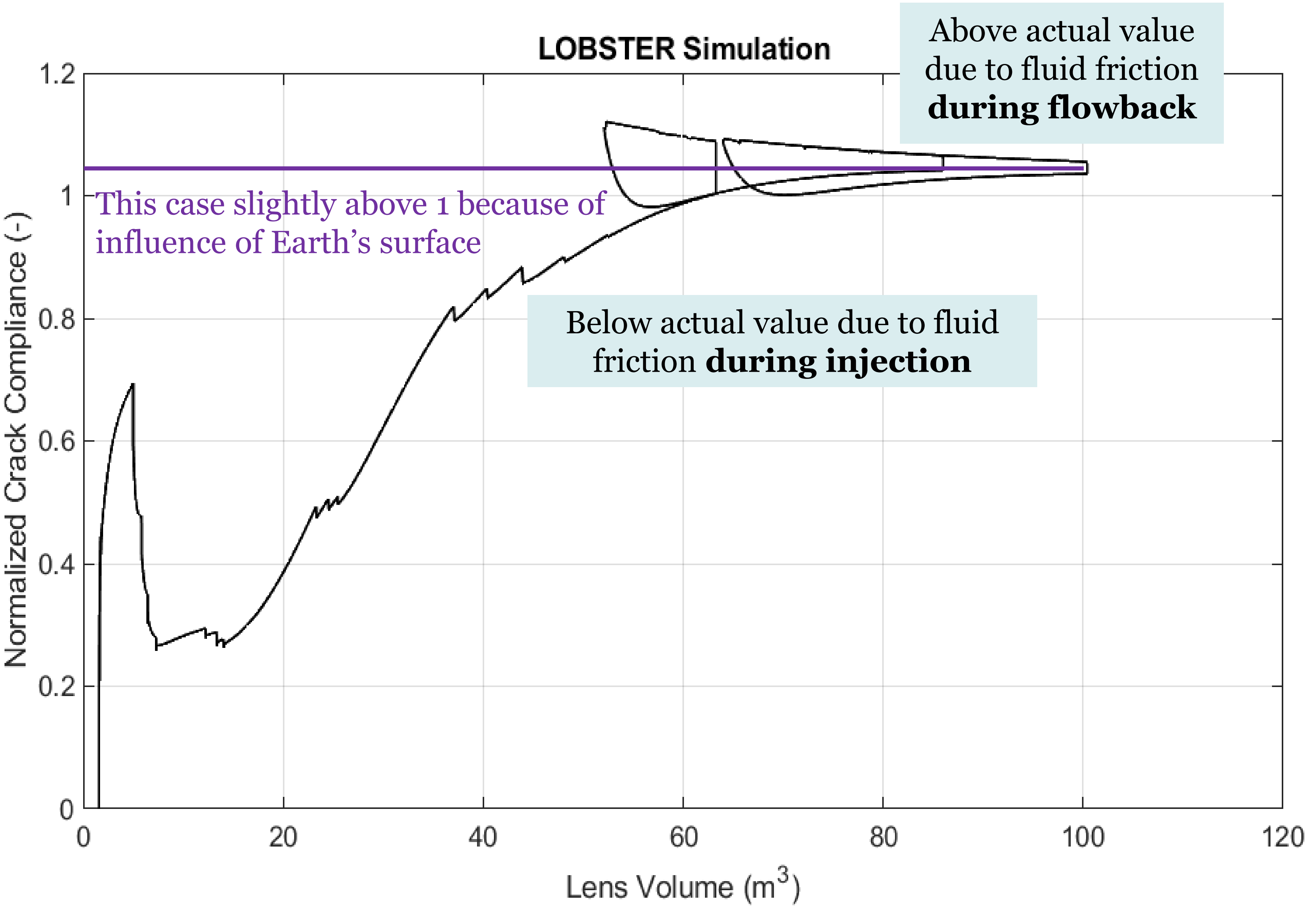

Case Study: Western Canadian Sedimentary Basin

- Create lens
  - Day 1: 1900 bbl (300 m^3) initial injection
  - Day 2: additional 400 bbl (65 m^3) injection
- Two months later, multiple reinflation and flowback cycles

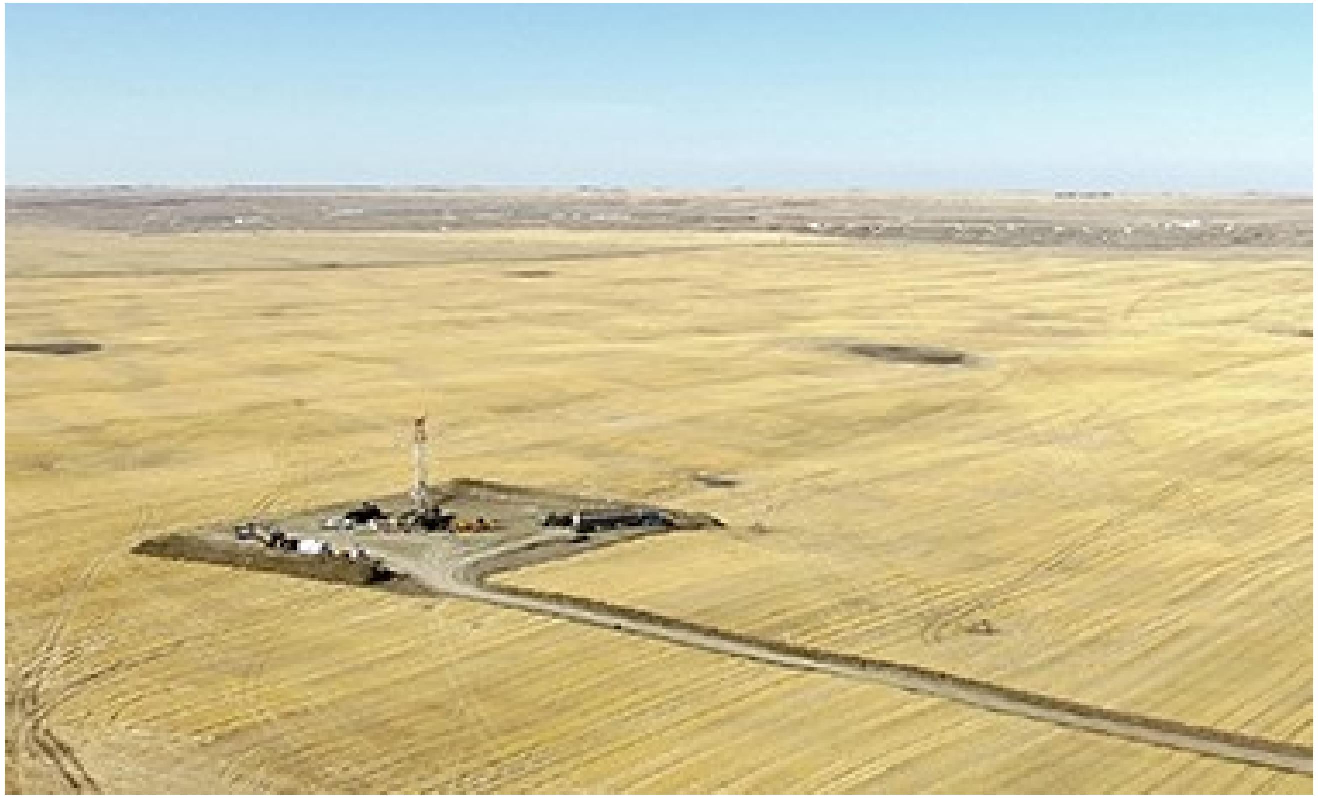

Injection and Flowback Test Cycles

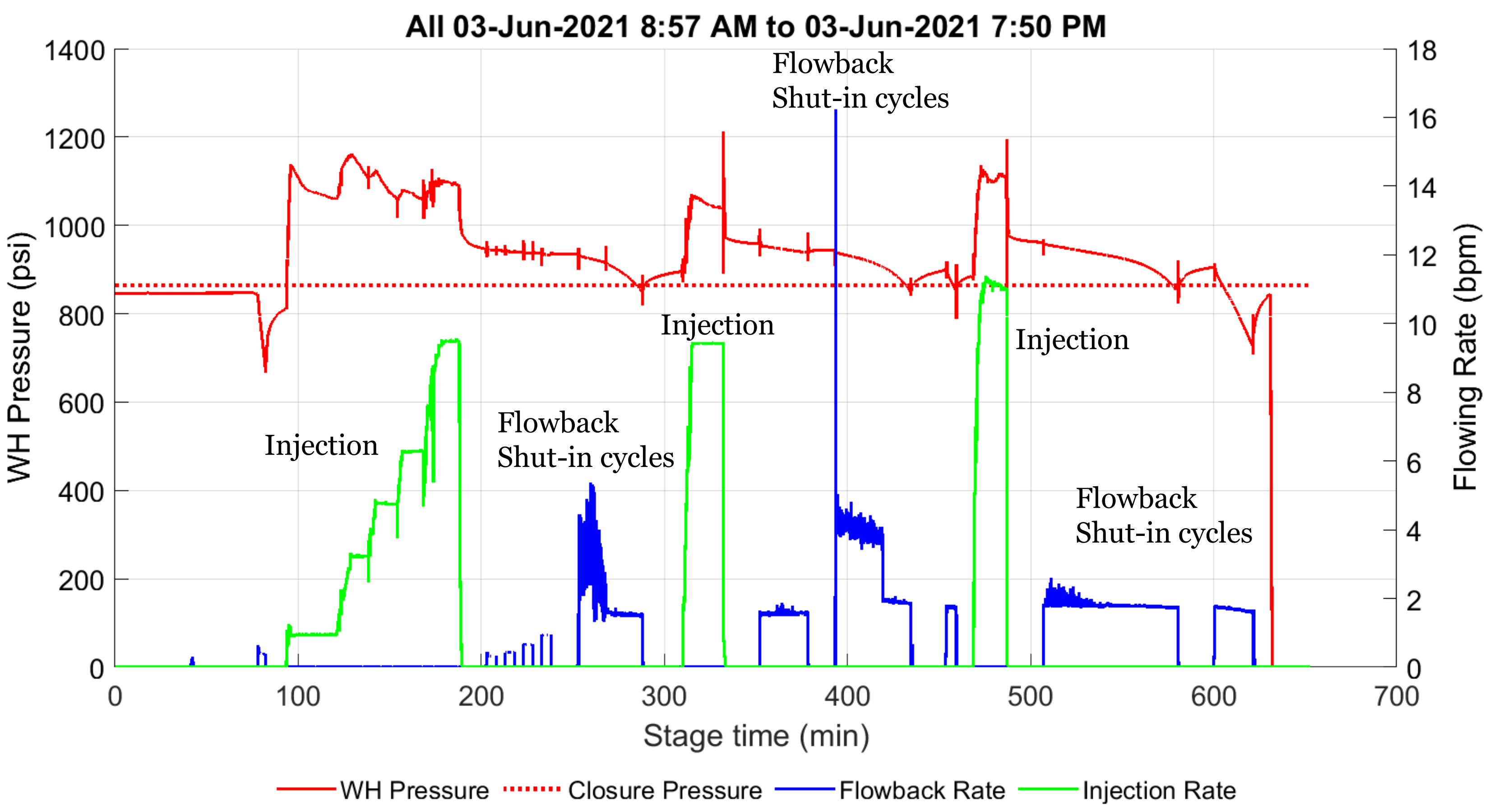

Summary:

- Flow #1
  - Drawdown to 4600 kPa (670 psi)
- Inflate #1
  - 64.2 m3, up to 1.5 m3/min
- Multichoke Test (MCT) #1
  - MCT 1a: 08/64" 5 mins, no pinch
  - MCT 1b: 10/64" 5 mins, no pinch
  - MCT 1c: 12/64" 5 mins, no pinch
  - MCT 1d: 16/64" 5 mins, no pinch
- Flow to pinch (FTP 1)
  - FTP 1a 18/64" 15 mins, no pinch, gasified
  - FTP 1b 20/64" 20 mins, imminent pinch
- Inflate #2
  - 1.5 m3/min for 30 m3
- FTP 2
  - FTP 2a: 20/64" 24 mins, no pinch
  - FTP 2b: 22/64" 40 mins, imminent pinch
  - FTP 2c: 22/64" 5 mins, imminent pinch
- Inflate #3
  - 2.0 m3/min for 30 m3
- FTP 3
  - FTP 3a: 22/64" 77 mins, imminent pinch
  - FTP 3b 22/64" 20 mins, imminent pinch

- Closure stress shown here for 1.07 psi/ft
- Flowback 1a, 2a, 2b, and 3a impacted by N_2 gas

Orientation and Shape from Tiltmeter Interpretation

- Tilt data indicative of horizontal (~10 deg dip) lens
- Extended Kalman Filter interpretation based on coupled planar hydraulic fracture model shows nearly circular shape

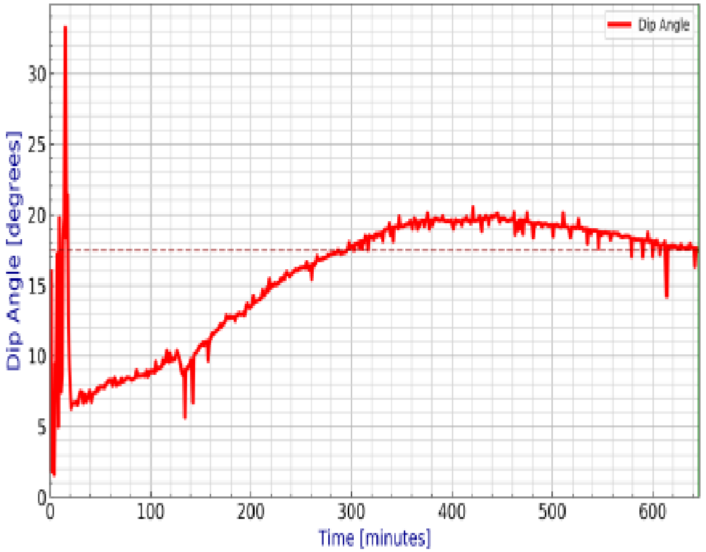

Inflate #3
30 m3

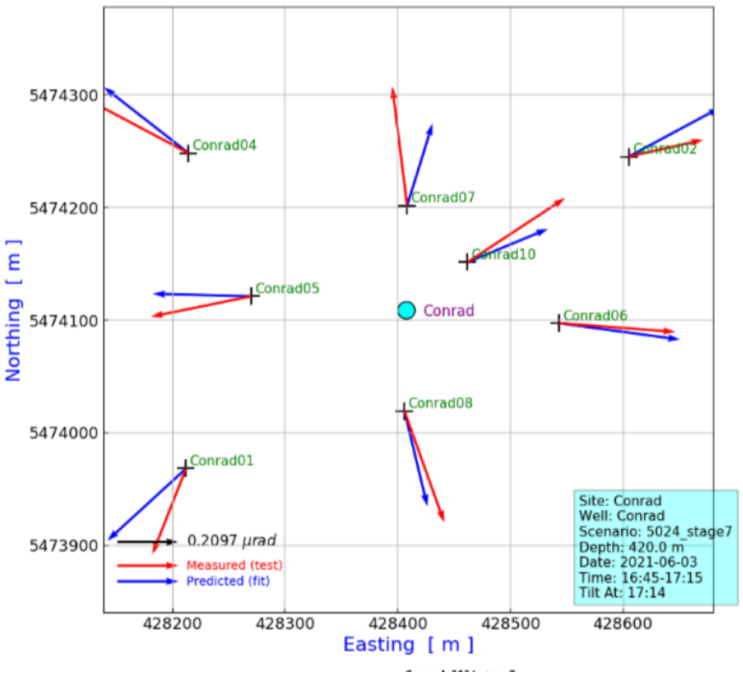

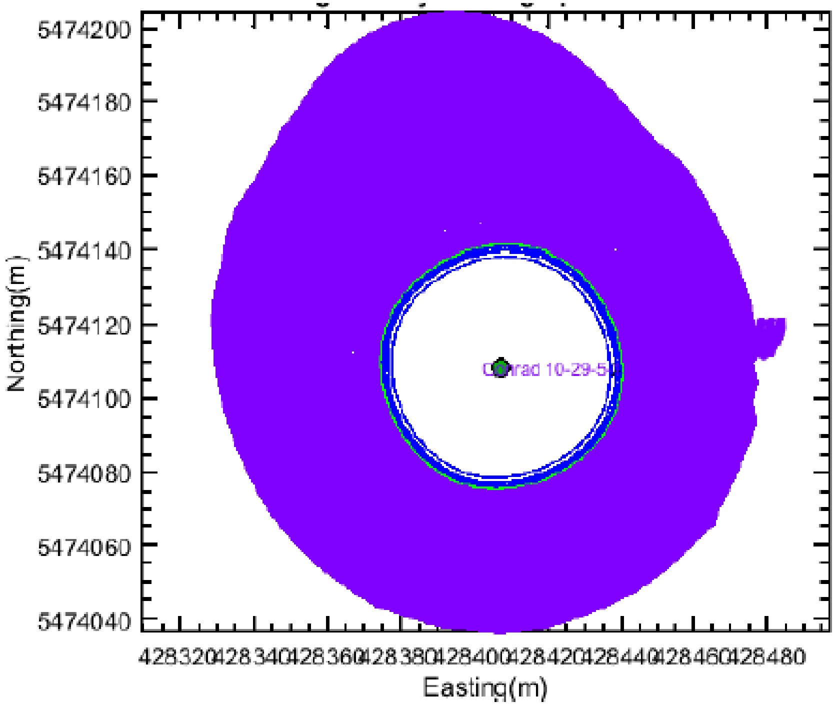

Tiltmeter Inferred Volumes

- Fluid leakoff 22% of total for first cycles, improves to 7% of total for later cycles
- Fluid efficiency improves from 78% to 93% with successive injections

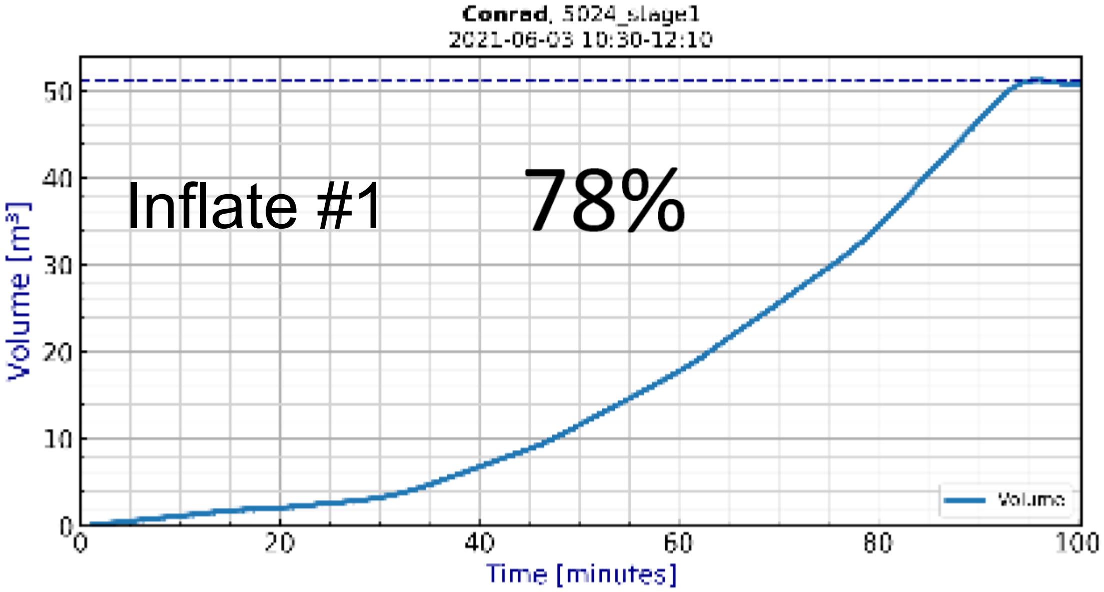

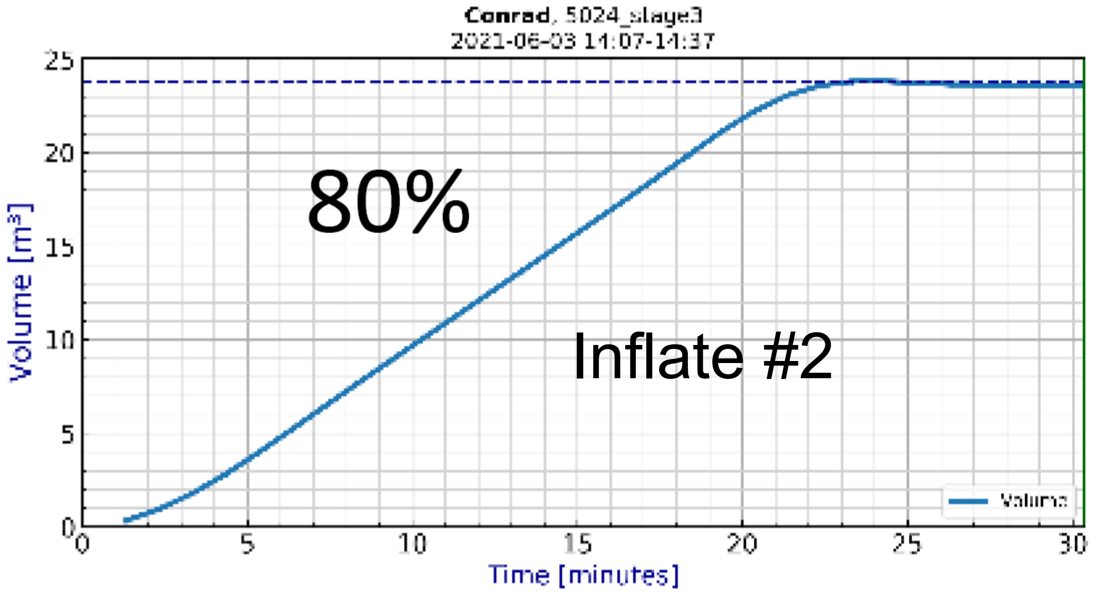

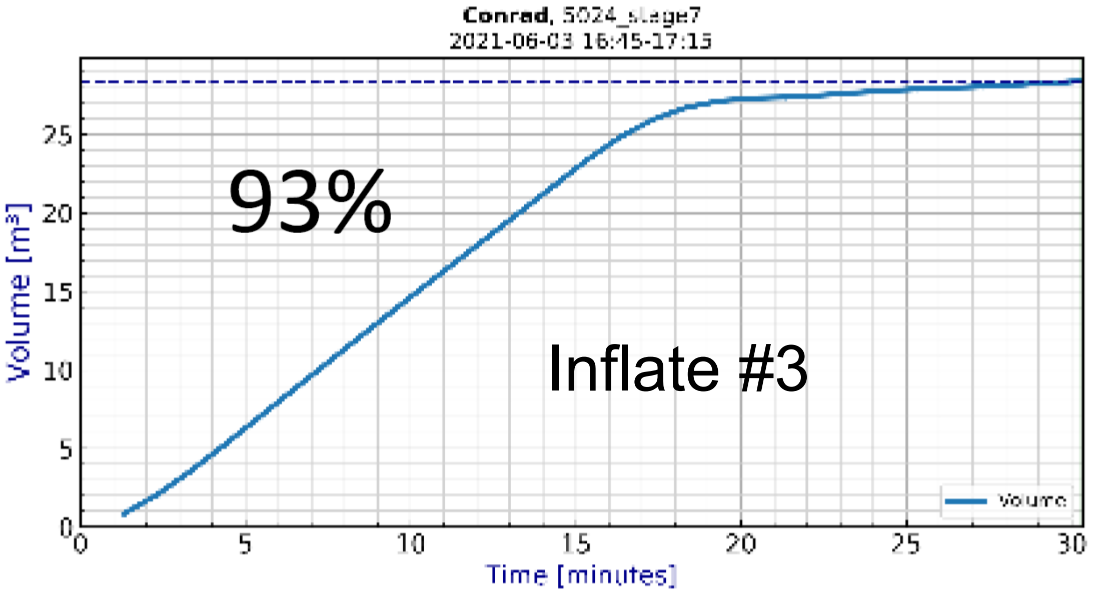

Caliper Lens Width Measurement at Wellbore

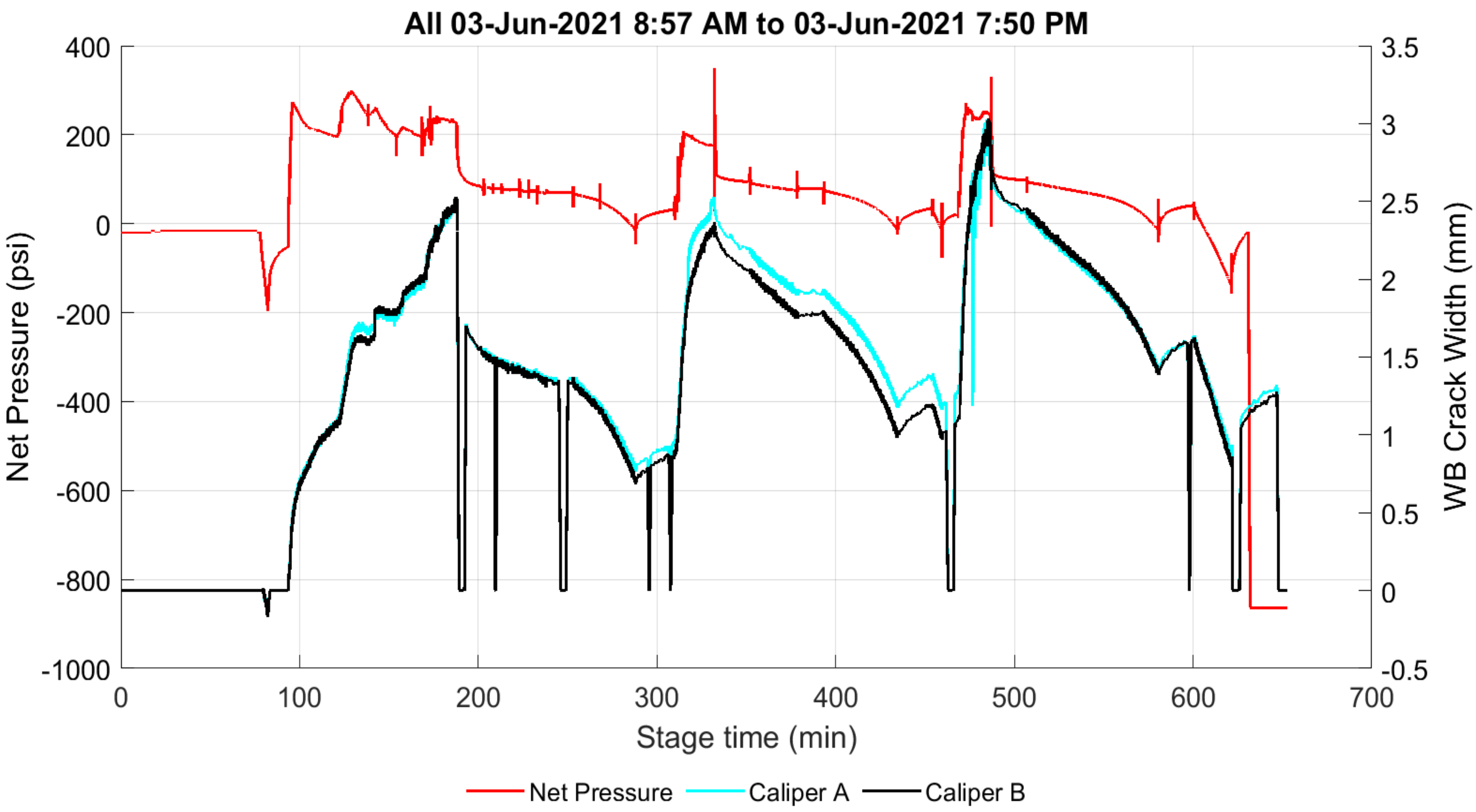

Field Measurement of Crack Compliance

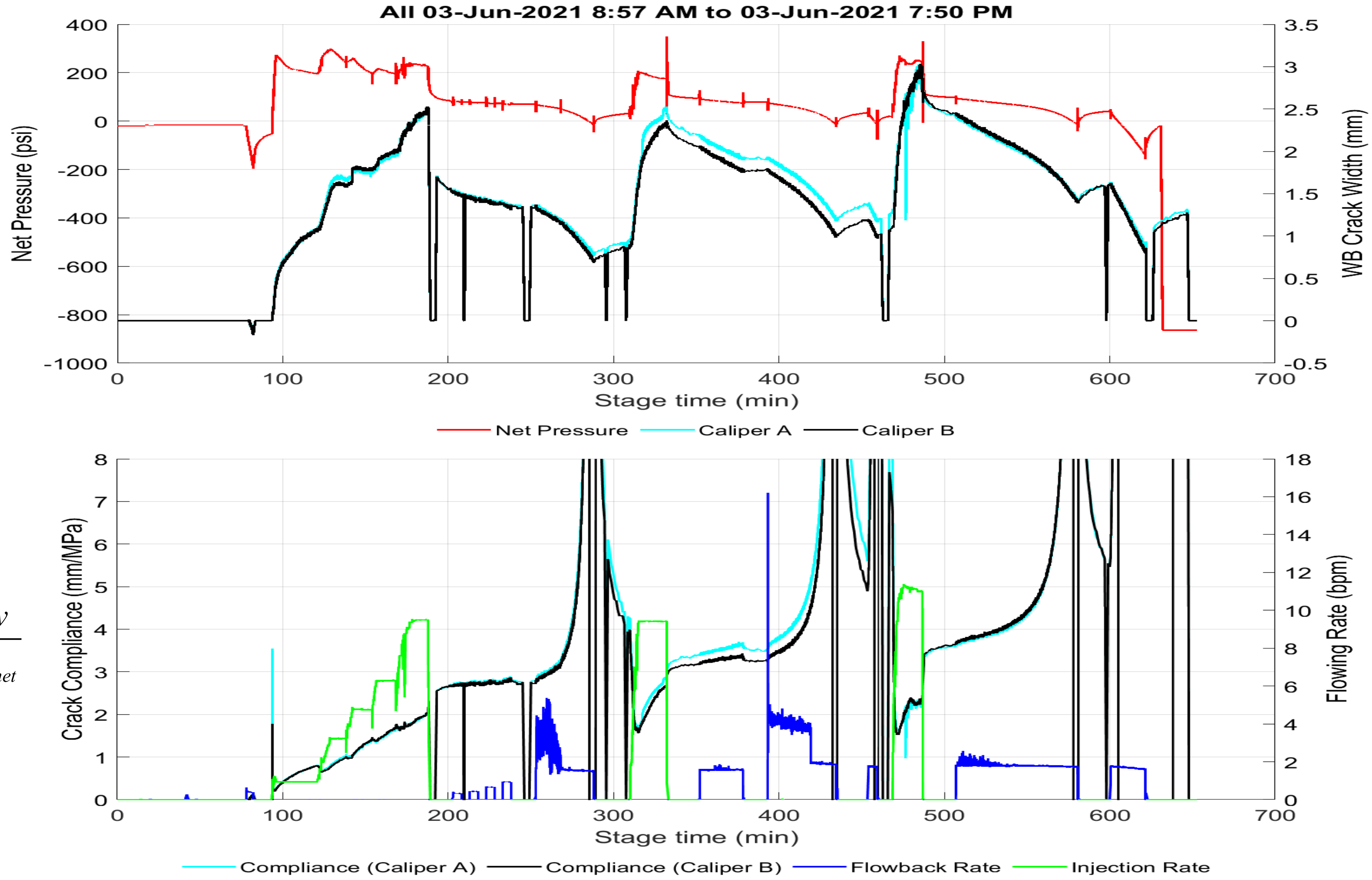

$$C = \frac{w}{p_{net}}$$

Field Compliance Compared to Elastic Compliance

Elastic Compliance:

$$V_{lens} = \frac{16 p_{net} R^3}{3E'}, \qquad w_o = \frac{8 p_{net} R}{\pi E'}$$

$$E' = \frac{E}{1-\nu^2}$$

$$\Rightarrow \frac{w_o}{p_{net}} = \frac{2^{5/3} 3^{1/3}}{\pi} \frac{V_{lens}^{1/3}}{E'^{2/3} p_{net}^{1/3}}$$

$$let: V_{lens} = \eta V_{inj}, \quad \boxed{E'_{app} = BE'_{meas}}$$

$$\chi = \frac{w_o}{\eta^{1/3} V_{inj}^{1/3}} \frac{E'^{2/3}}{p_{net}^{2/3}} \frac{\pi}{2^{5/3} 3^{1/3}} = \boxed{\frac{1}{B^{2/3}}}$$

Apparent elastic stiffness is around 8x higher than sonic log value of 15 GPa

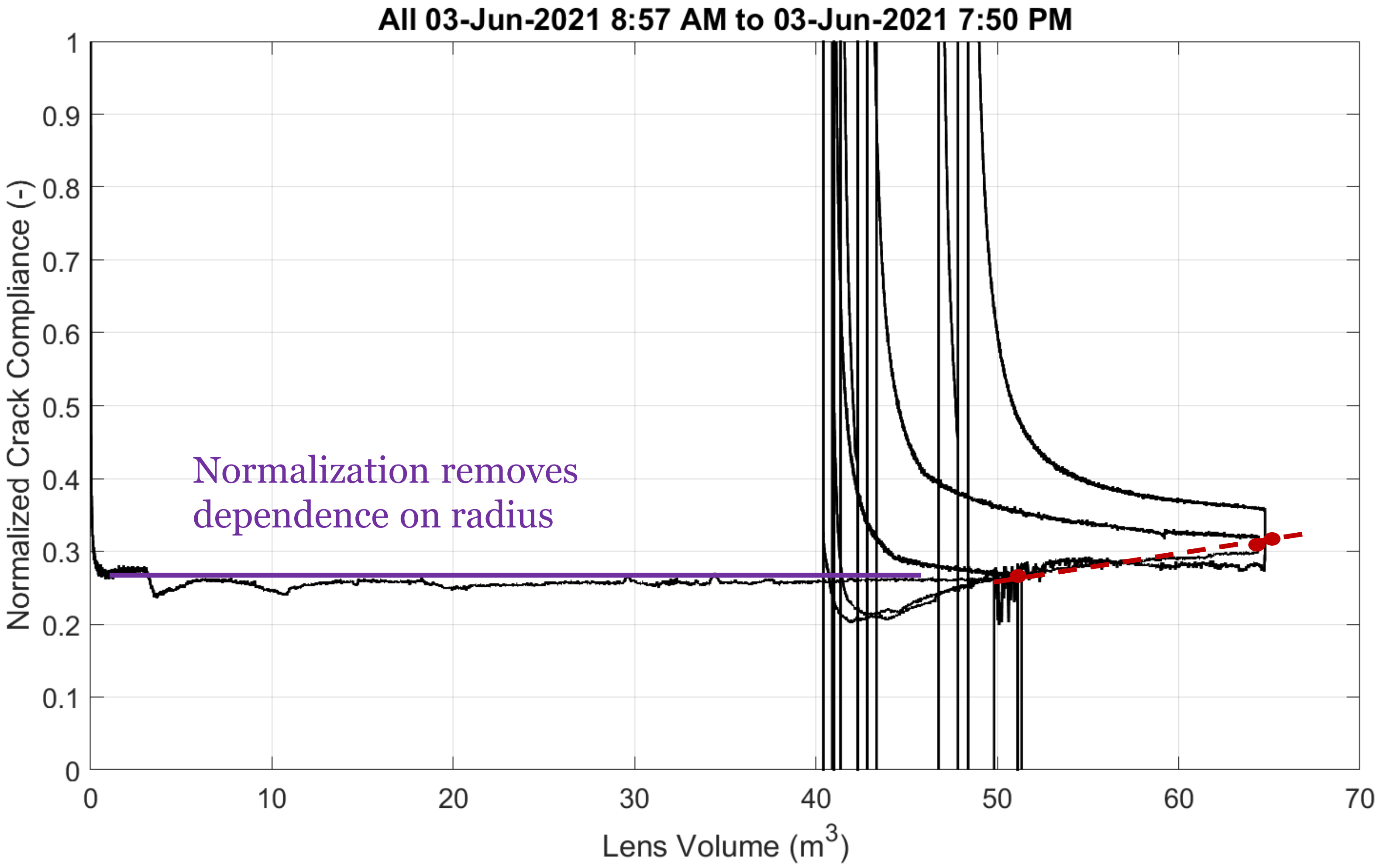

Upward trend of compliance with multiple cycles – in LOBSTER this is captured by bridge breaking

Bridge Connections – Geological Evidence and Model

- Segmentation with subsequent overlap leads to bridges
- Continued inflation can break bridges

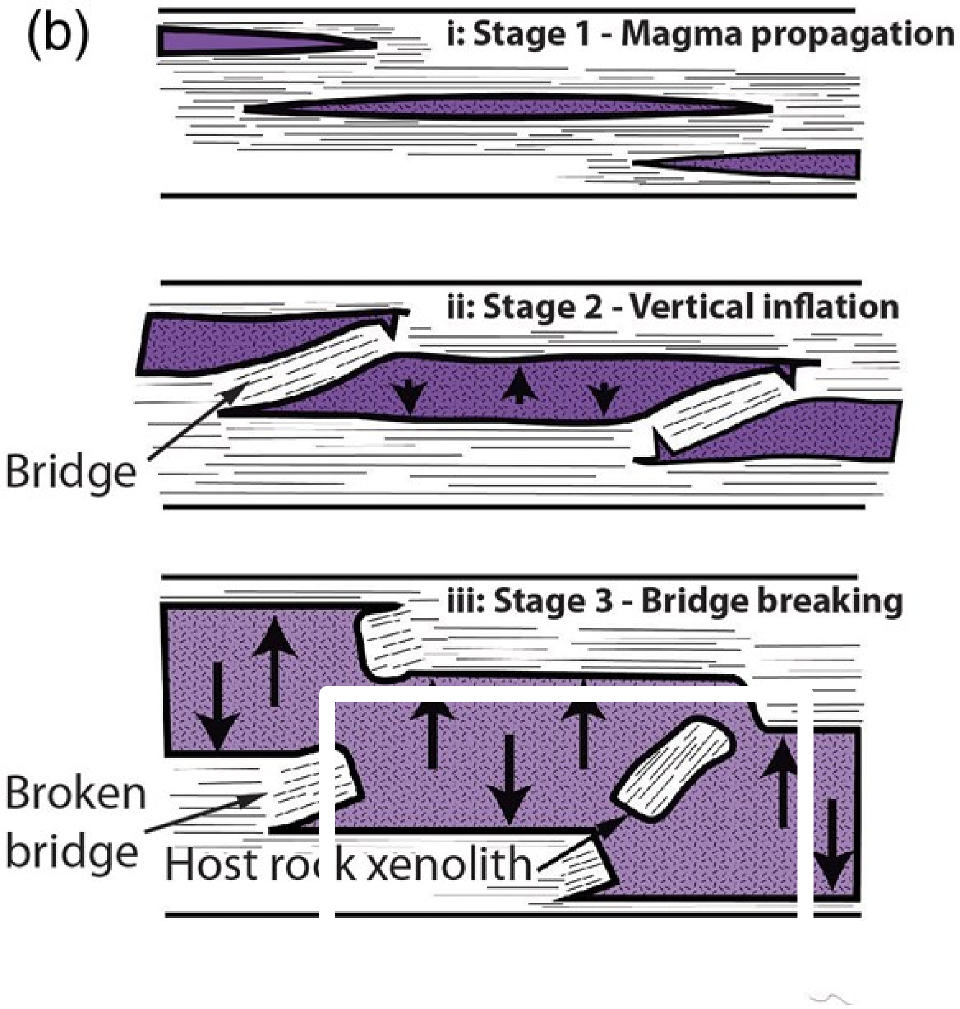

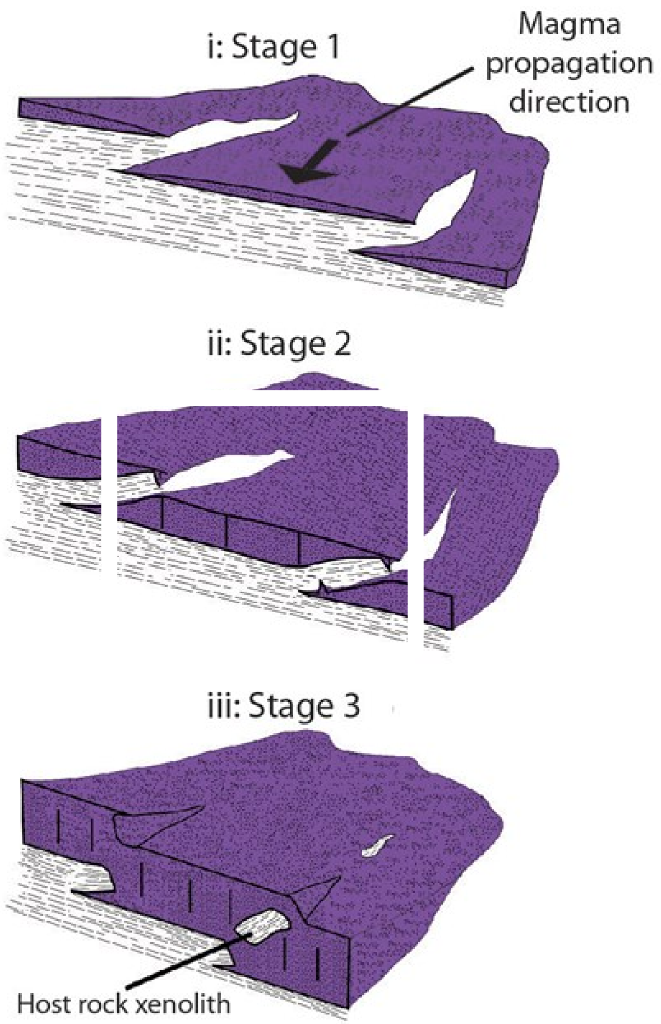

Eide, C. H., Schofield, N., Jerram, D. A., & Howell, J. A. (2017). Basin-scale architecture of deeply emplaced sill complexes: Jameson Land, East Greenland. *Journal of the Geological Society*, *174*(1), 23-40.

Bridge Connections – Geological Evidence and Model

- Segmentation with subsequent overlap leads to bridges
- Continued inflation can break bridges

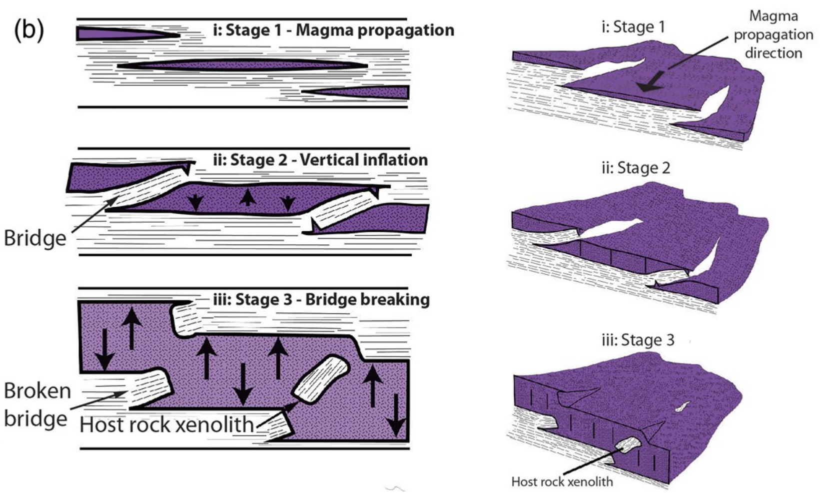

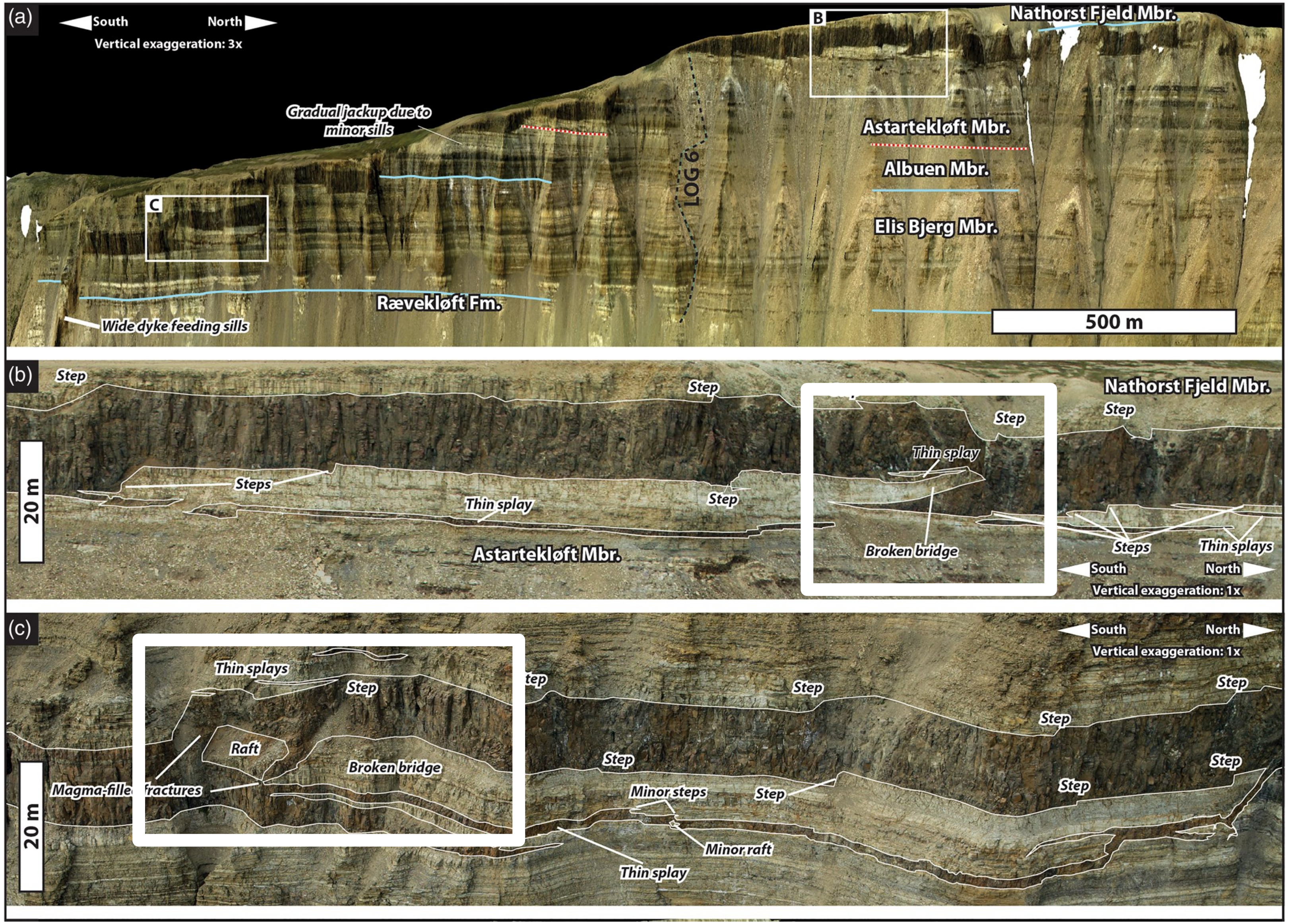

Eide, C. H., Schofield, N., Jerram, D. A., & Howell, J. A. (2017). Basin-scale architecture of deeply emplaced sill complexes: Jameson Land, East Greenland. *Journal of the Geological Society*, *174*(1), 23-40.

Bridge Connections – Evidence at Lab Scale

- Crack front bifurcation during growth leads to segmentation and hence intact rock bridges cutting through the lens
- Could act like tension springs that stiffen the lens, making it less compliant

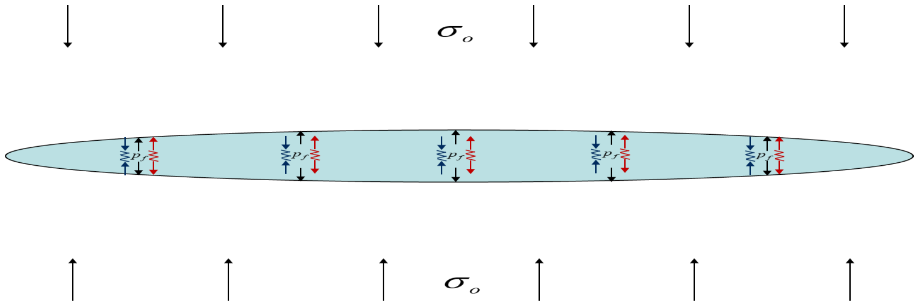

Ruiting Wu, PhD Thesis, 2006 (Georgia Tech).

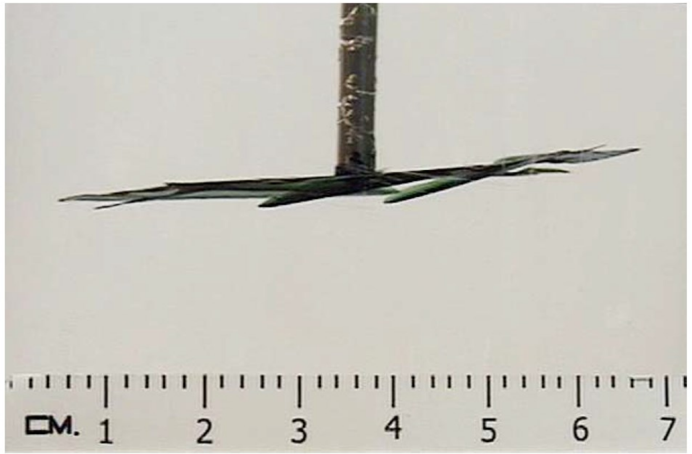

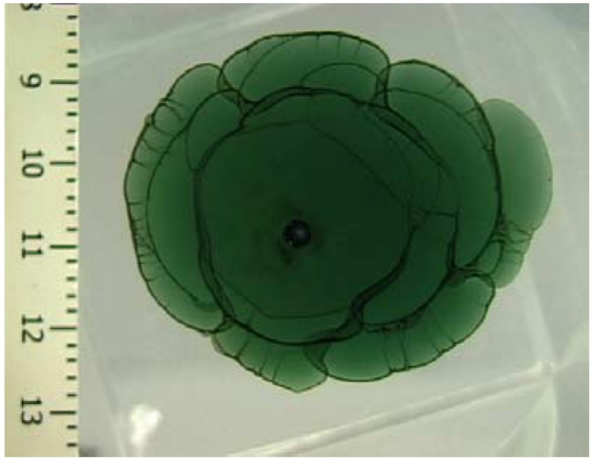

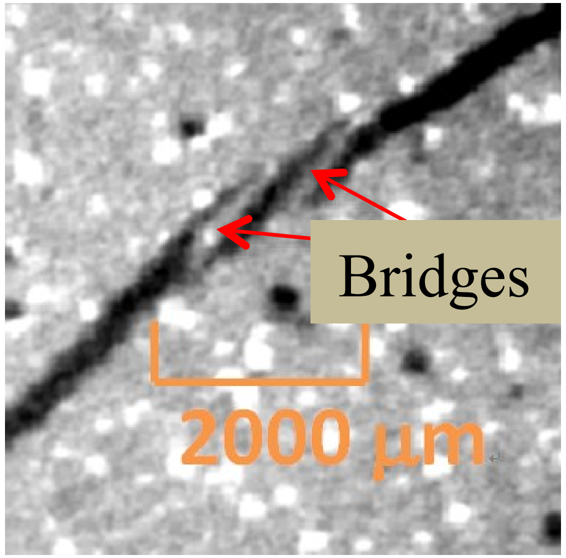

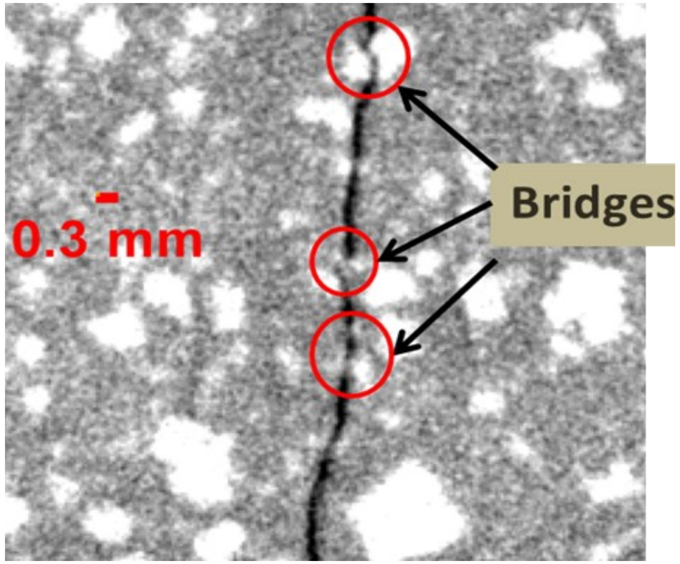

Dyskin, A.V., E. Pasternak, J. He, M. Lebedev & B. Gurevich, 2016. The role of bridge cracks in hydraulic fracturing. In: Proc. 10th Int. Conf. on Structural Integrity and Failure (SIF2016), Kotousov A, Ma J (eds), Adelaide, Australia, 2016, Paper #6.
He, J., E. Pasternak, A.V. Dyskin, M. Lebedev & B. Gurevich, 2017b. The constricted effect of bridges in hydraulic fracturing. ACAM 9.

Bridge Condition

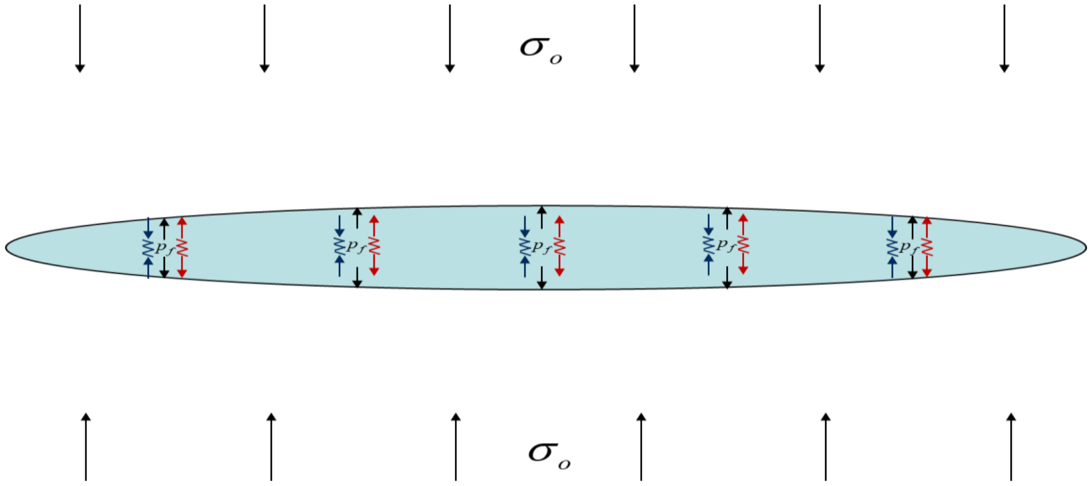

$$p_{f,i} - \sigma_o = -\frac{E'}{R}\sum_{j=1}^{m} A_{ij} w_j - s_i(w_i)$$

$$s(w) = E\left[-\eta_T \left|\frac{w_T - w_{\max}}{w_T}\right|^{\alpha_T} \frac{w}{w_T} \hat{H}\left(w_T - w_{\max}\right)\right]$$

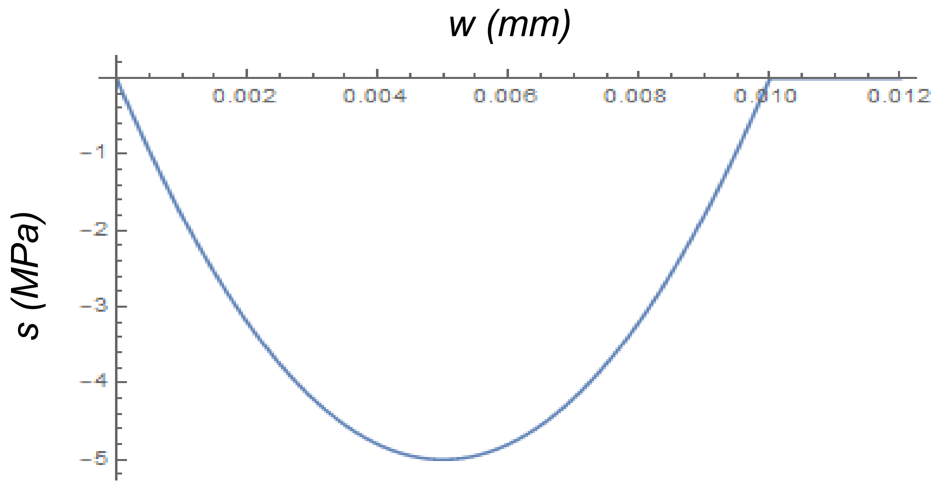

Bridges:

- Linear elastic stretching of bridges
- Non-linear decrease of bridge area as bridges permanently break
- History dependence – solution "remembers" largest width ever attained at each location
- Result: Increasing tension as width increases, and then decreasing tension as bridges break

Bunger, A. P., Lau, H., Wright, S., & Schmidt, H. (2023). Mechanical model for geomechanical pumped storage in horizontal fluid-filled lenses. International Journal for Numerical and Analytical Methods in Geomechanics, 47(8), 1349-1372.

Field Data Indication of Bridges: Conrad LC5 Example

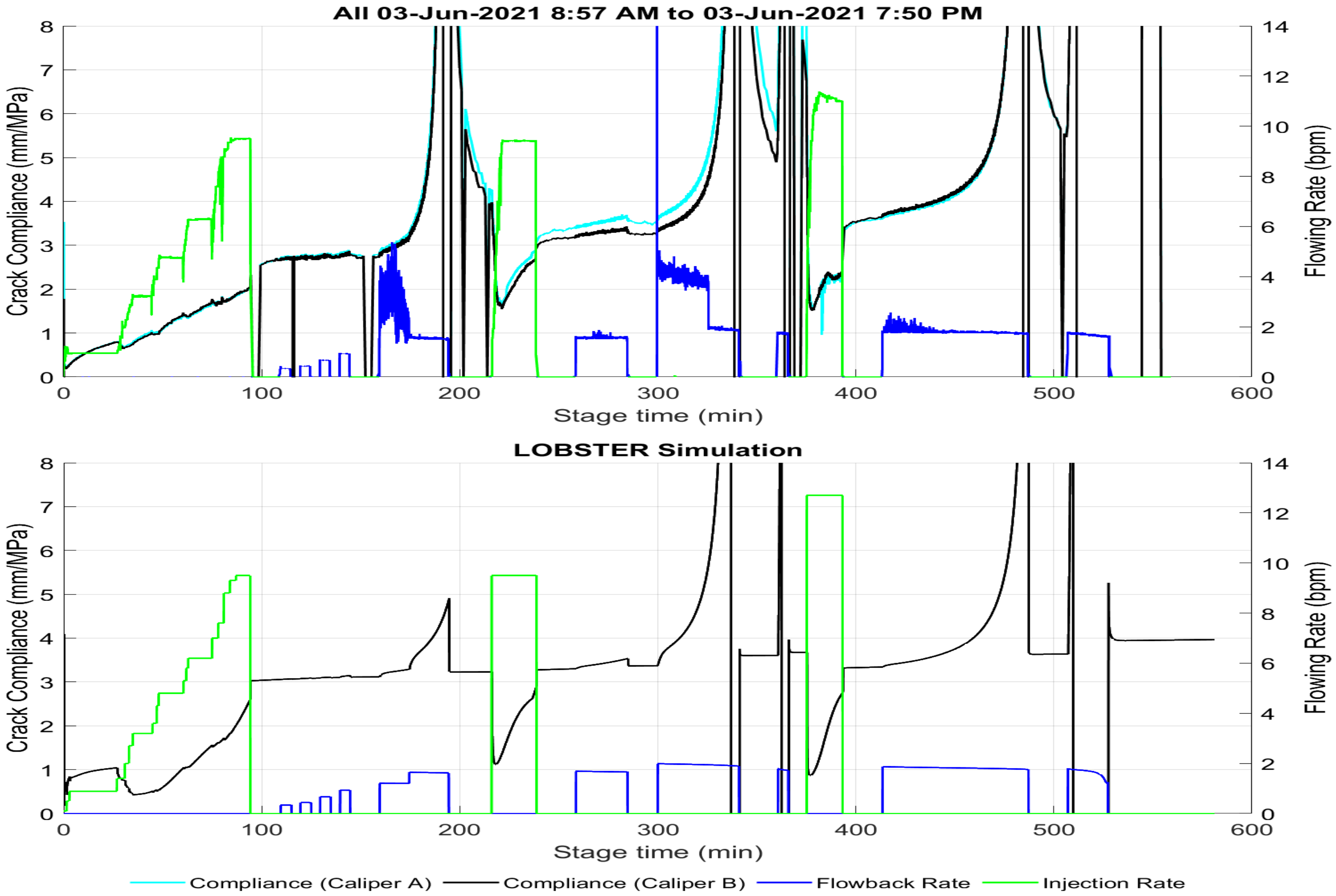

Field Data Indication of Bridges: Conrad LC5 Example

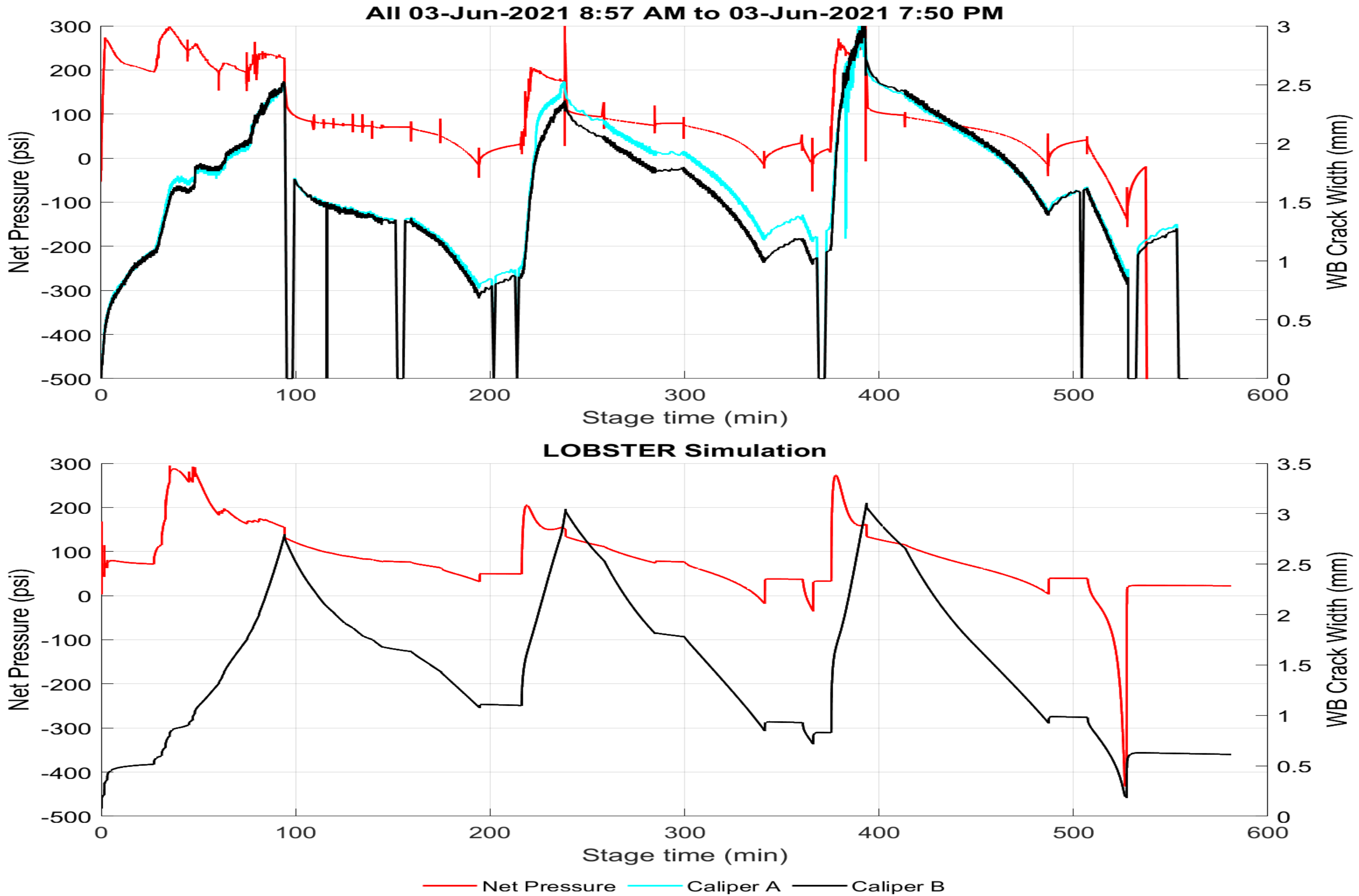

Fit between Model and Data: MCT1a

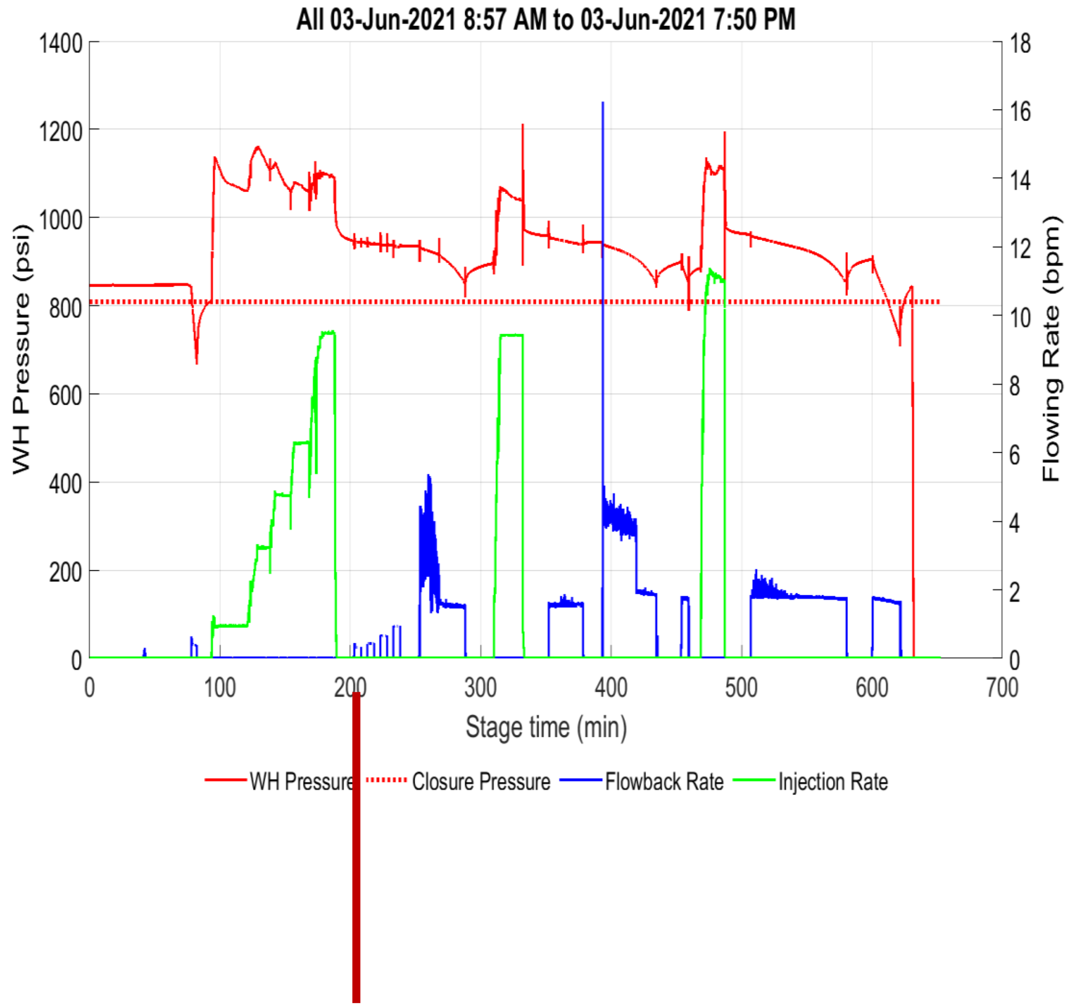

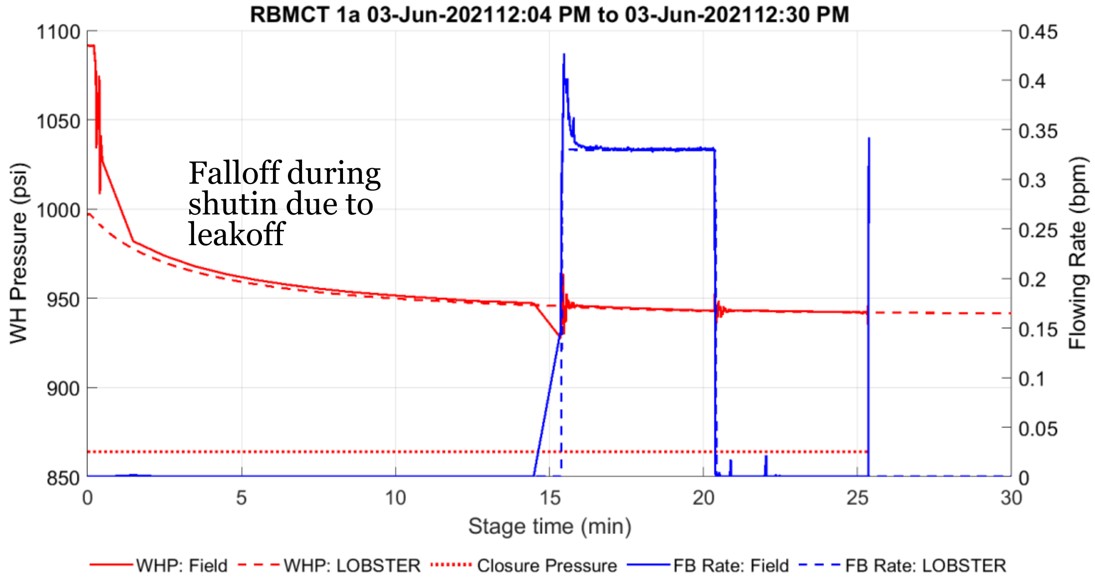

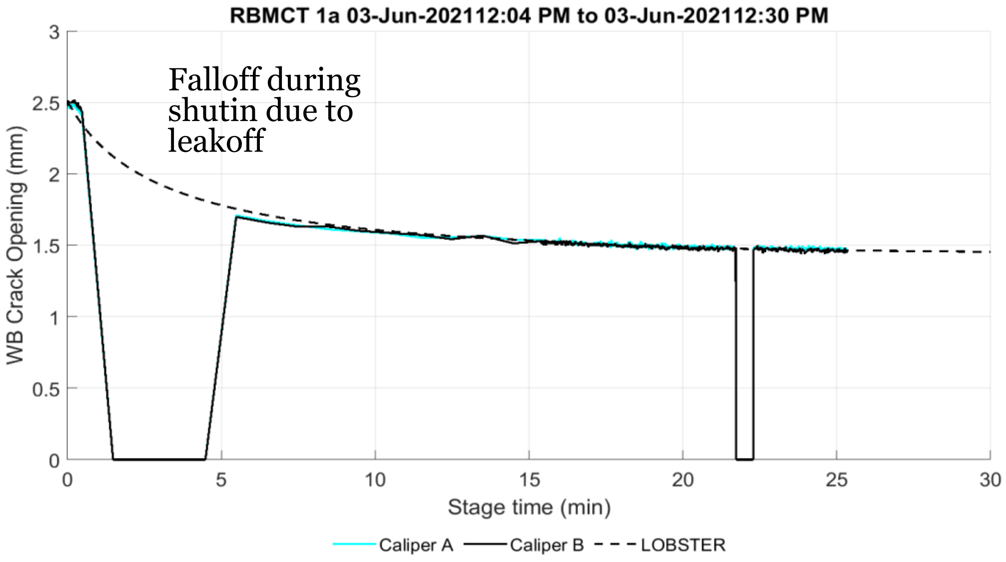

Goodness of Fit between Model and Data

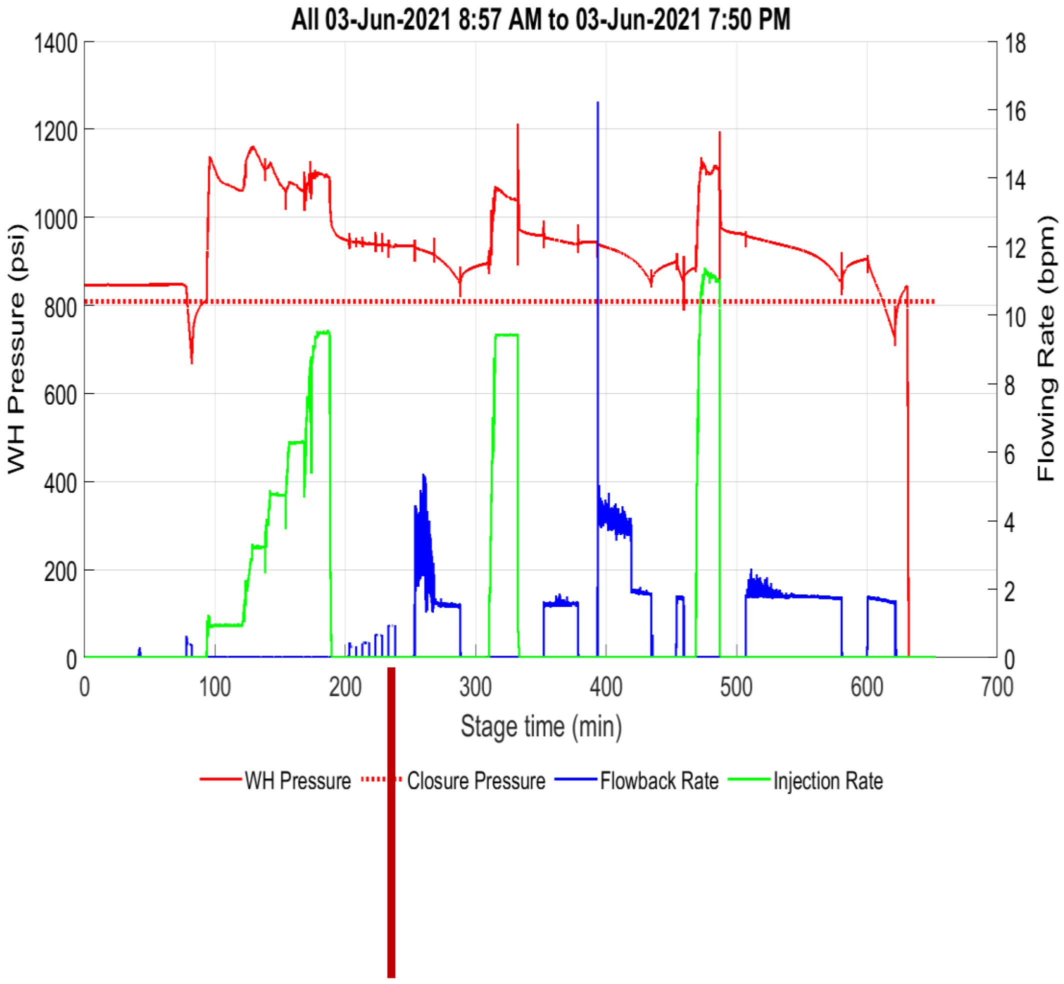

Prediction versus data

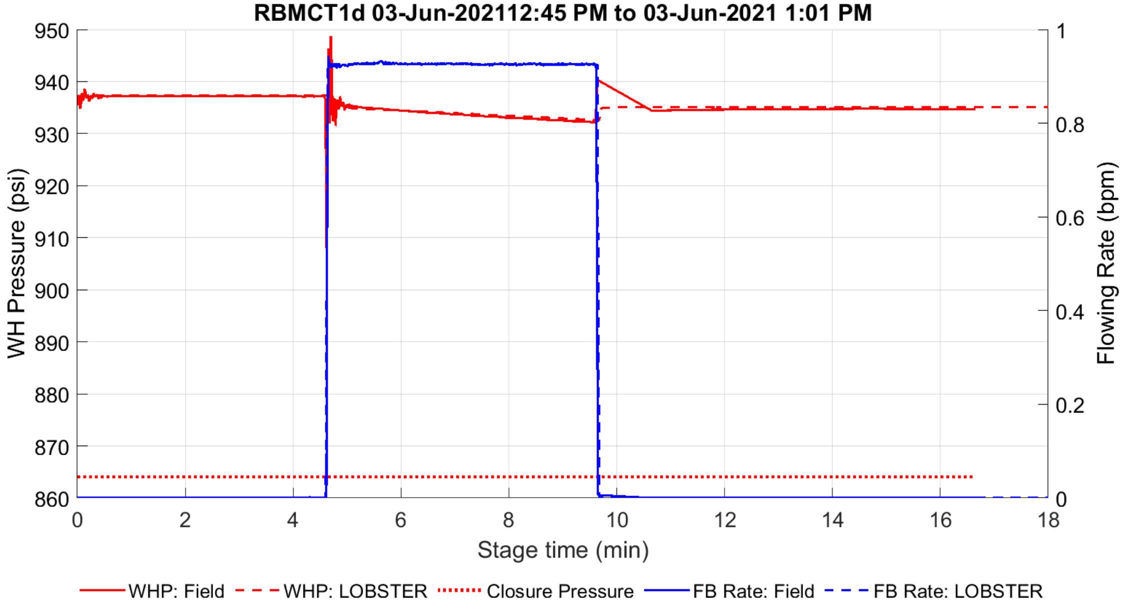

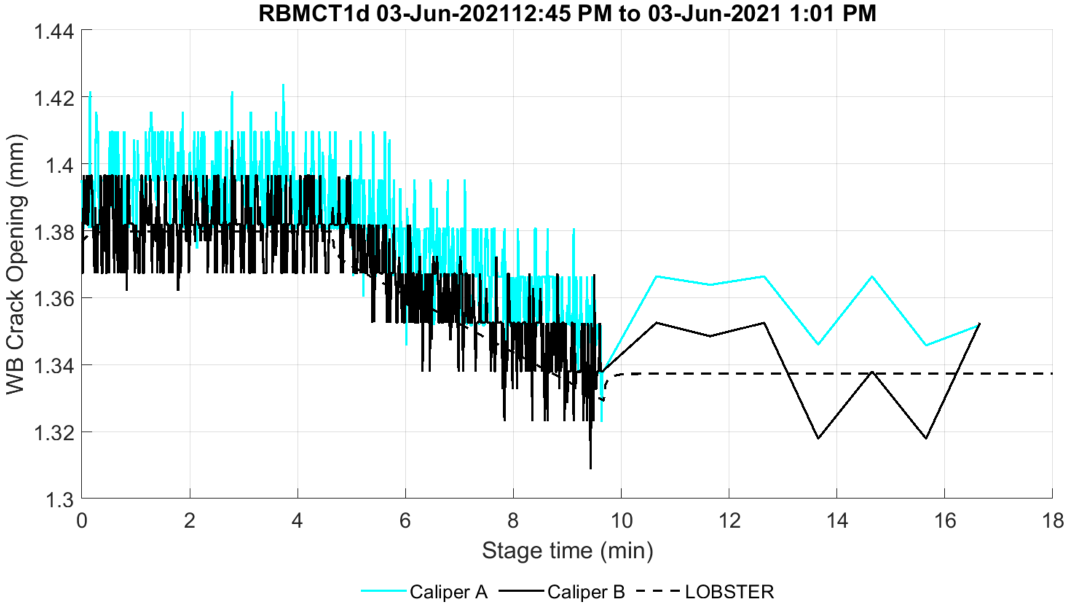

Goodness of Fit between Model and Data

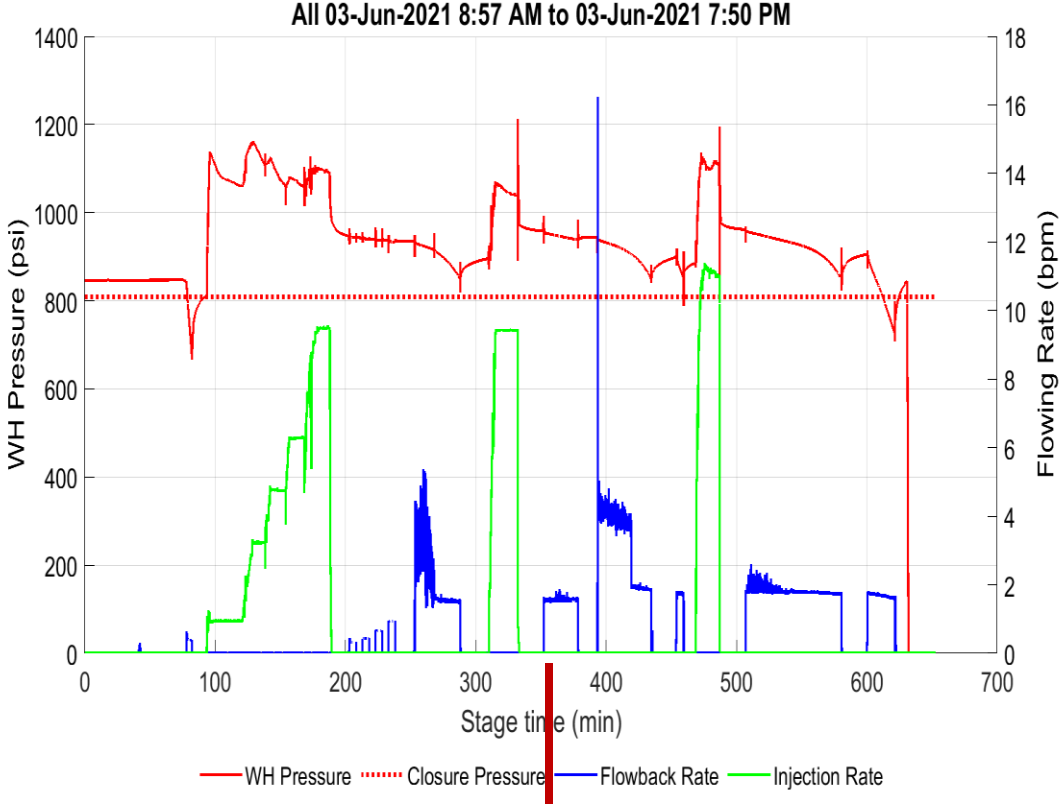

Prediction versus data

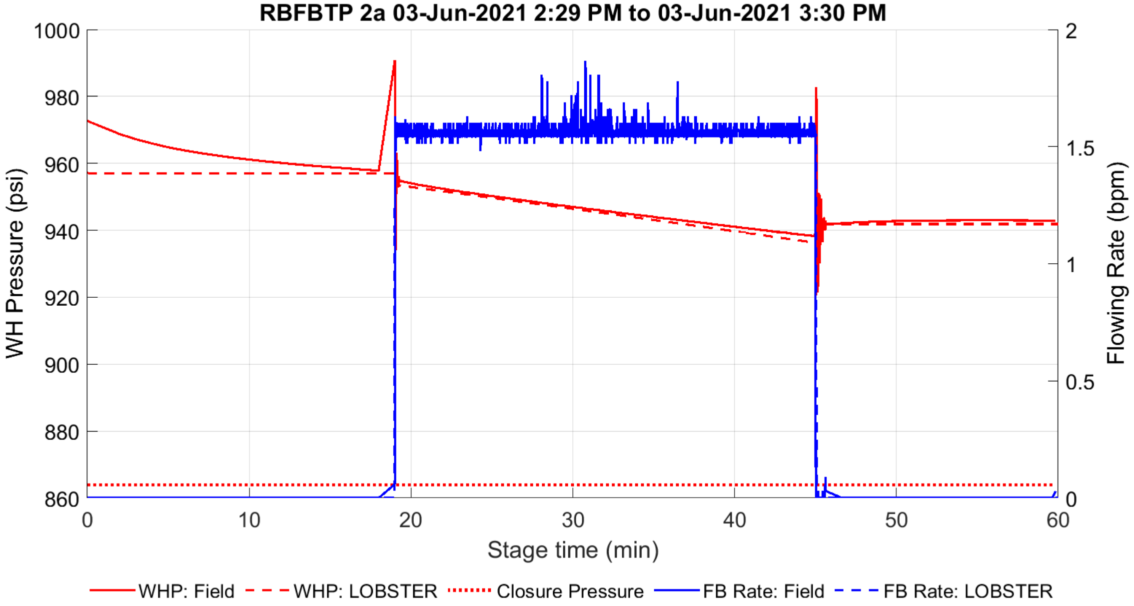

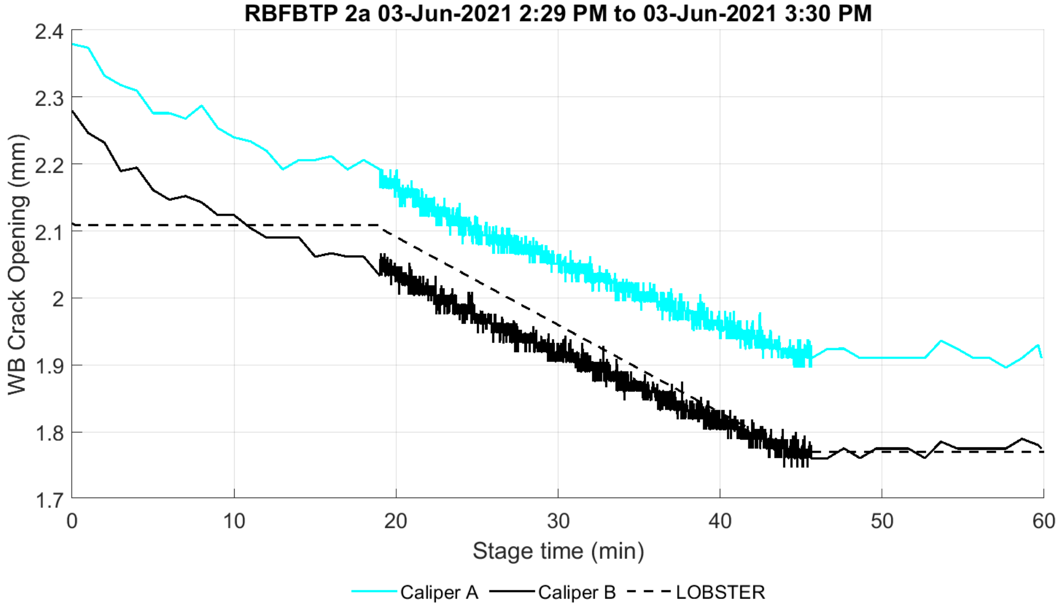

Fit between Model and Data: FBTP2b

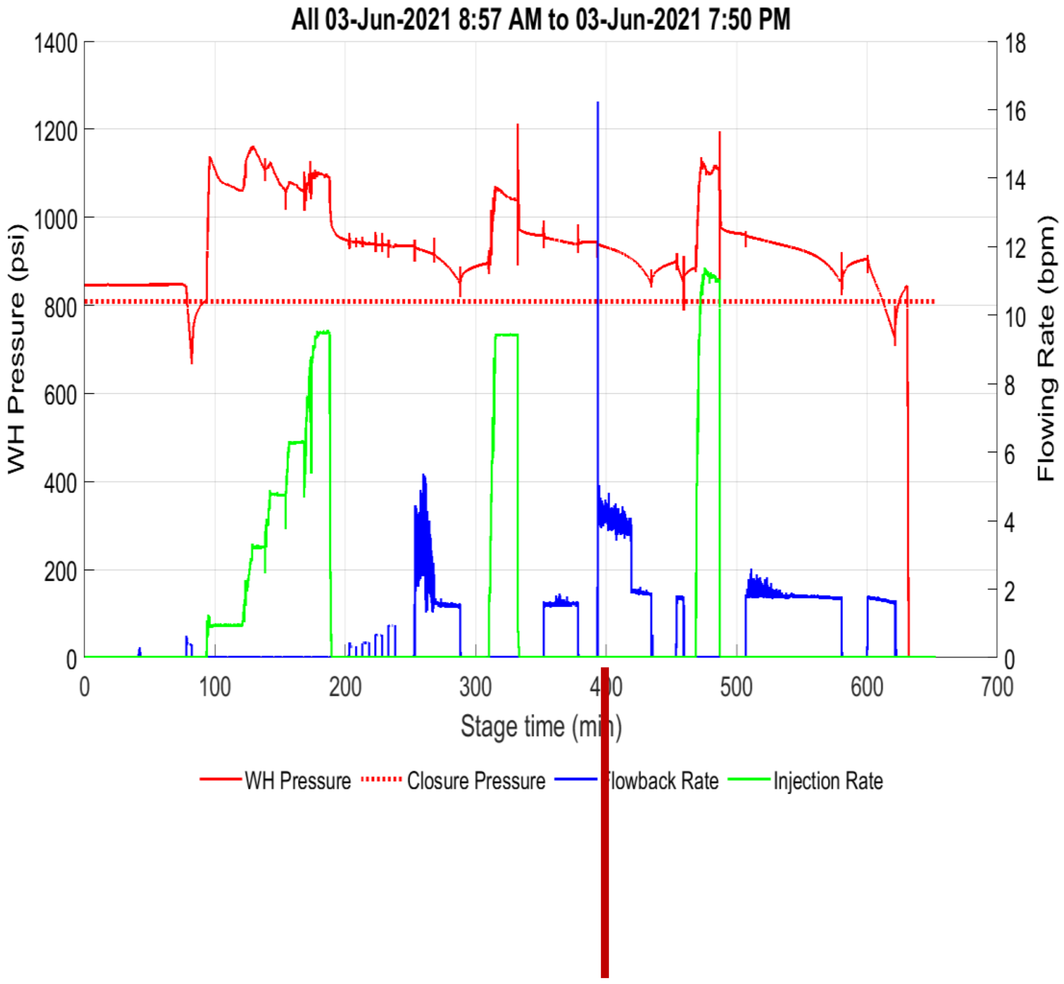

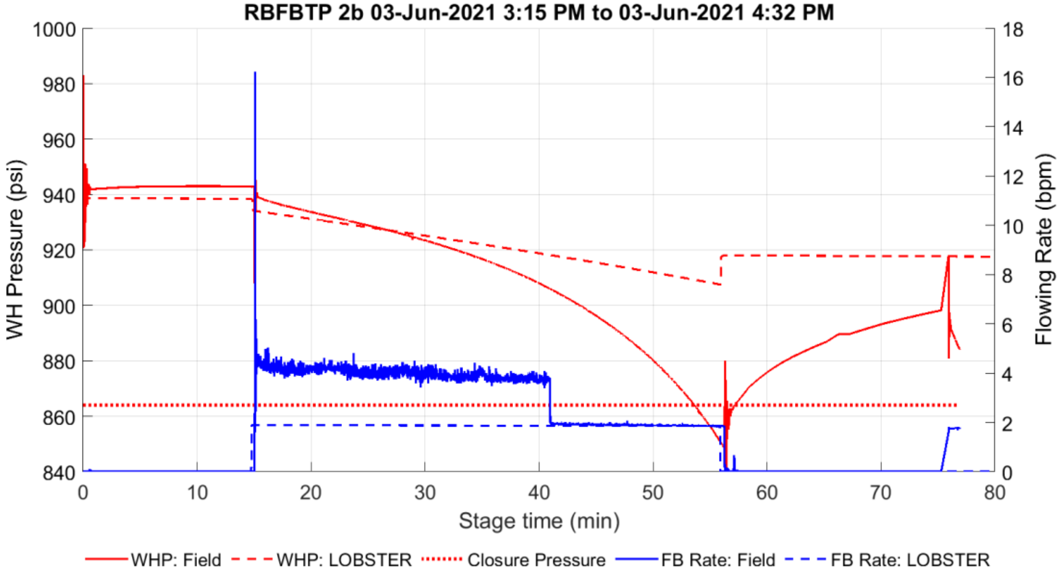

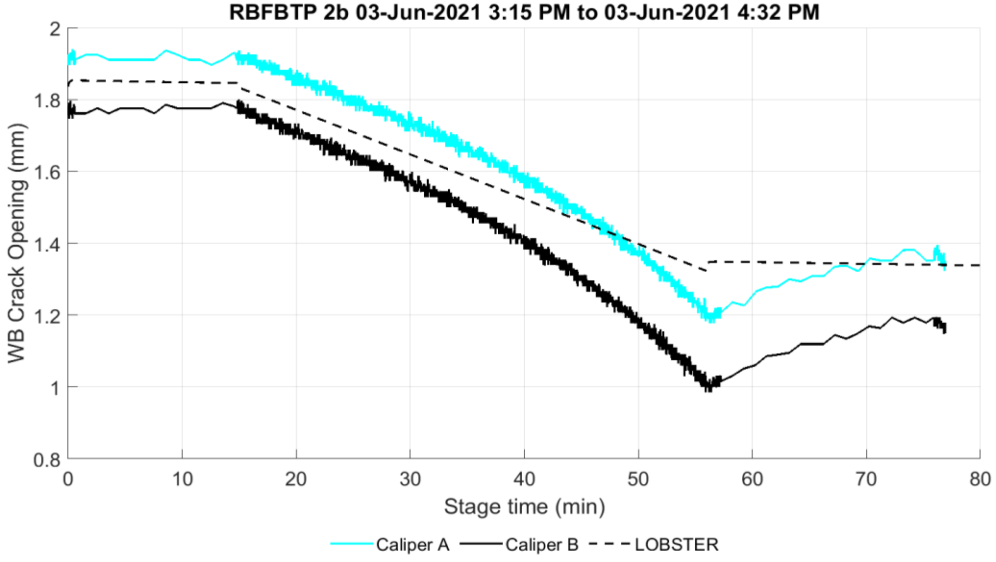

Conclusions

- Fluid-solid coupling in tip region leads to asymptotic behavior distinct from LEFM
- Rock failure is time-dependent
  - Failure can occur at load levels well below what is required for instantaneous failure
  - Acoustic emission signature shows coalescence of microcracks in leadup to failure
  - Aftershocks are generated from vicinity of failure surface
- Rock fracture involves segmentation resulting in intact bridges
  - Crack compliance is far below prediction from LEFM
  - Will lead to underprediction of pressure and length and overprediction of width when not accounted for in models

Acknowledgments

- Funding and permission to present field test data from Quidnet Energy
- Tiltmeter inversion/interpretation from CSIRO Energy
- Discussion of bridges (prior to this project) with Arcady Dyskin and Elena Pasternak (University of Western Australia), as well as a travel grant for APB from the Australian Research Council (as a part of DP190103260)